T.C.
ISTANBUL AYDIN UNIVERSITY
INSTITUTE OF GRADUATE STUDIES

SOLAR AND WIND BASED HYBRID ENERGY SYSTEM IN NIGERIA

MASTER'S THESIS

Eromosele Oziegbe IHONGBE

Department of Mechanical Engineering
Energy Technologies Program

AUGUST, 2023

T.C.
ISTANBUL AYDIN UNIVERSITY
INSTITUTE OF GRADUATE STUDIES

SOLAR AND WIND BASED HYBRID ENERGY SYSTEM IN NIGERIA

MASTER'S THESIS

Eromosele Oziegbe IHONGBE
(Y2112.023001)

Department of Mechanical Engineering
Energy Technologies Program

Thesis Advisor: Prof. Dr. Mehmet Emin TACER

AUGUST, 2023

APPROVAL PAGE

DECLARATION

I hereby declare with the respect that the study “Solar and Wind Based Hybrid Energy System in Nigeria”, which I submitted as a Master thesis, is written without any assistance in violation of scientific ethics and traditions in all the processes from the project phase to the conclusion of the thesis and that the works I have benefited are from those shown in the References. (31/8/2023)

Eromosele Oziegbe IHONGBE

FOREWORD

First, I would like to express my endless gratitude to God for being who I am right now and helping me to find patience, strength within myself to complete this thesis.

I would also like to thank my family not only for encouraging me to go abroad for a master's degree but also for teaching me to chase my dreams and never give up.

I would also like to extend my sincere appreciation to my supervisor, Prof. Dr. MEHMET EMIN TACER, for his exceptional expertise, patience, and unwavering commitment to academic excellence. His guidance, insightful feedback, and continuous support have been invaluable throughout this journey.

Prof. Dr. MEHMET EMIN TACER is not only professional in his field, but a person with a great heart that keeps encouraging me.

Finally, I would like to acknowledge the important contribution of Istanbul Aydin University to my life, not only from an academic perspective but helping to meet great people that inspire, challenge, support and motivate me.

August, 2023 Eromosele Oziegbe IHONGBE

SOLAR AND WIND BASED HYBRID ENERGY SYSTEM IN NIGERIA

ABSTRACT

The increasing demand for electricity in Nigeria has prompted a strong focus on clean and sustainable energy sources, leading to a significant interest in the integration of solar and wind-based hybrid energy systems.

Furthermore, this study explores the very important considerations in the system design for solar and wind-based hybrid energy systems in Nigeria. It discusses various system configurations, with a focus on grid-connected systems. It emphasizes the significance of efficient energy conversion technologies, such as photovoltaic panels and wind turbines, to maximize power generation and overall system efficiency.

Various Simulations were carried out using MATLAB like evaluating the accuracy and responsiveness of the P&O MPPT method in tracking solar irradiation, the simulation used a step time of 0.1 and assumed irradiance levels ranging from 200 to 1000 W/m2. the voltage profile of the connected and unconnected Hybrid-Grid Network was analysed and compared for the 33Kv, 132kv and the 330kv, the observed line losses for the Grid network were also analysed for both the connected and un-connected Hybrid system and studying the impact of a percentage load increase of 20%, 60%, and 100% on the hybrid-grid operating at 33kV.

I also used the Mat lab Simulink application to test the system control loop for the wind energy and we have shown the results in this Study.

In conclusion, this study deals with the challenges and solutions connected to the grid integration of solar and wind-based hybrid energy systems into the existing Nigerian power grid.

Keywords: Marketing Strategy, Nestle, SWOT, PESTLE, Financial analysis

NİJERYA'DA GÜNEŞ VE RÜZGAR TABANLI HİBRİT ENERJİ SİSTEMİ

ÖZET

Nijerya'da elektriğe olan talebin artması, temiz ve sürdürülebilir enerji kaynaklarına güçlü bir odaklanmayı tetikledi ve bu da güneş ve rüzgar bazlı hibrit enerji sistemlerinin entegrasyonuna önemli bir ilgi duyulmasına yol açtı.

Ayrıca, bu çalışma Nijerya'daki güneş ve rüzgar bazlı hibrit enerji sistemleri için sistem tasarımındaki çok önemli hususları araştırmaktadır. Şebekeye bağlı sistemlere odaklanarak çeşitli sistem konfigürasyonlarını tartışır. Enerji üretimini ve genel sistem verimliliğini en üst düzeye çıkarmak için fotovoltaik paneller ve rüzgar türbinleri gibi verimli enerji dönüştürme teknolojilerinin önemini vurguluyor.

MATLAB kullanılarak, güneş ışınımının izlenmesinde P&O MPPT yönteminin doğruluğunun ve duyarlılığının değerlendirilmesi gibi çeşitli Simülasyonlar gerçekleştirilmiş, simülasyonda 0,1'lik bir adım süresi kullanılmış ve 200 ila 1000 W/m2 arasında değişen ışınım seviyeleri varsayılmıştır. bağlı ve bağlantısız Hibrit Şebeke Ağının voltaj profili analiz edildi ve 33Kv, 132kv ve 330kv için karşılaştırıldı, Şebeke ağı için gözlemlenen hat kayıpları hem bağlı hem de bağlantısız Hibrit sistem için de analiz edildi ve etkinin incelenmesi 33kV'de çalışan hibrit şebekede yüzde 20, %60 ve %100 oranında yük artışı.

Ayrıca rüzgar enerjisi için sistem kontrol döngüsünü test etmek amacıyla Matlab Simulink uygulamasını kullandım ve sonuçları bu çalışmada gösterdim.

Sonuç olarak bu çalışma, güneş ve rüzgar bazlı hibrit enerji sistemlerinin mevcut Nijerya elektrik şebekesine şebeke entegrasyonuyla bağlantılı zorluklar ve çözümleri ele alıyor.

Anahtar Kelimeler: Pazarlama Stratejisi, Nestle, SWOT, PESTLE, Finansal analiz

TABLE OF CONTENTS

DECLARATION ..... **i**
FOREWORD ..... **ii**
ABSTRACT ..... **iii**
ÖZET ..... **iv**
TABLE OF CONTENTS ..... **v**
LIST OF ABBREVIATIONS ..... **vii**
LIST OF TABLES ..... **x**
LIST OF FIGURES ..... **xi**
I. INTRODUCTION **1**
A. Introduction 1
1. The Current Status of the National Grid 33, 330 and 132 KV in Nigeria's. 1
2. Renewable Energy in Nigeria 2
II. CHAPTER TWO **4**
A. Solar Energy 4
1. Solar Photovoltaic System 5
2. PV System Components 5
3. Analysis of the Solar System 6
4. Mathematical Model of Photovoltaic Array 6
B. Maximum Power Point Tracking 10
C. DC-DC Boost Converter Model 12
D. Average Model of a DC-AC Inverter 14
III. CHAPTER THREE **16**
A. Simulation Results 16
1. MPPT (Perturb and Observe algorithm) 16
2. DC-AC Inverter and DC-DC Boost Converter 18
3. Conclusions 20
IV. CHAPTER FOUR **22**
A. Wind Power 22

1. Component of a wind energy project 23
B. Introduction to Wind Energy 24
1. Wind Energy System Composition 25
C. Converter Model Considered 27
1. The Control Topologies for Converters 28
2. Filter Model Used 29
3. Control Loops 30
D. Conclusion 35
V. CHAPTER FIVE 36
A. Modelling and Simulation of Wind and Solar Based Hybrid Energy System 36
1. Integrated 330 Kv Power System Buses 37
B. Simulation of Wind and Solar Power 39
1. Wind Energy System 41
2. The voltage profile of the connected and unconnected Hybrid-Grid Network was analysed and compared. 42
3. Scenario Two 44
4. Scenario Three 47
5. Summary 49
VI. CONCLUSION 53
VII. REFERENCES 55
RESUME 61

LIST OF ABBREVIATIONS

Base Case : Initial condition or reference state of a power system

DFIG : Doubly Fed Induction Generator

DG : Distributed Generation

Ema : mean annual solar radiation, kWh/m2

Ep : estimated peak energy delivered, kWh

GFG : Gas-fired Generator

I : current through load, A

Id : current through diode, A

IEEE : Institute of Electrical and Electronics Engineers

Ii : i-th Line Current

Impp : current at maximum power, A

Io : reverse saturation current, V

Ipv : current generated by PV, A

Isc : short circuit current, A

Ish : current through the shunt resistor, A

k : Boltzmann's constant = (1.3806488×10−23), J.K-1

kWp : nominal peak energy, kW

MVA : Mega Volt Ampere

n : linearity factor (1 for ideal diode)

n : number of modules

ng : Number of generators

p.u : Per Unit

PGi : i-th conventional generator's capacity

PGinew : i-th generator's new capacity after wind penetration

Phydro **: Hyd**ro plants' equivalent real power

Pi : Real power flow on the i-th line

Ploss : Real power loss

Pmax : maximum power, W

PMSG : Permanent Magnetic Synchronous generator

PQ Bus : Bus with specified active and reactive power injections

Ptherm : Thermal plants' equivalent real power

PV Bus : Bus with specified active power injection and voltage magnitude

PV : Photovoltaic

Pw : Wind turbine's real power

q : elementary charge= (1.602176565×10−19), C

Qi : Reactive power flow on the i-th line

RE : Renewable Energy

Ri : i-th Line Resistance

RL : Resistance-Inductance

Rs : equivalent circuit series resistance, Ω

Rsh : equivalent circuit shunt resistance, Ω

T : p-n junction absolute temperature, K

Tc : temperature of the PV cell, K

Tstc : temperature of STC, 25 °C, K

U : voltage applied to the load, V

Umpp : voltage at maximum power, V

Uoc : open circuit voltage, V

Ush : shunt voltage, V

Vi : i-th line's voltage drop

VT : thermal voltage,

Wp : peak energy of a single module, W

WTG : Wind Turbine Generator

X : Line reactance

η : efficiency of system

ϒ : power temperature coefficient, °C-1

LIST OF TABLES

Table 1. Electrical data of ph0t0voltaic module 7
Table 2. Boost Parameter 31
Table 3. PMSG parameters 32
Table 4 Integrated 330kv Power System Buses 37
Table 5 Bus Network Transmission Line 37
Table 6. Load Data 39

LIST OF FIGURES

Figure 1. 52-bus 0ne line diagram of the 33O kV Nigerian p0wer grid 2
Figure 2. S0lar and Wind Energy System [34] 3
Figure 3.S0lar system 4
Figure 4. Schematic diagram of the s0lar system 5
Figure 5. Block diagram of a basic grid-connected PV system 6
Figure 6 Equivalent circuit of the one-diode PV cell 8
Figure 7. PV array subsystem Simulink 8
Figure 8. Inside the PV array subsystem 9
Figure 9. PV module Vpv output voltage calculation 10
Figure 10. Characteristic PV array power curve 2] 10
Figure 11. Flowchart of the implemented P&O alg0rithm 12
Figure 12. PV system with MPPT C0ntr0l 12
Figure 13. Circuit of a DC-DC boost converter 13
Figure 14. Average model of DC-DC Boost converter 14
Figure 15. Average m0del 0f single-phase DC-AC Inverter 15
Figure 16. PV array current acc0rding t0 time for vari0us irradiance value 16
Figure 17. MPPT P-V curve (s0lid line) and P-V curve (dashed line) for vari0us irradiance value 17
Figure 18. MPPT P-V AND P-I curves (dashed lines and Sold Lines) for difference irradiance 17
Figure 19. MPPT c0ntr0l, PV array, DC-AC inverter, DC-DC c0nverter and Final M0del 18
Figure 20. DC-DC b00st Converter Output Voltage 19
Figure 21. AC current (red) and AC Voltage (blue) according to time 20
Figure 22. Output (red) and Input (blue) Power for the DC-AC Inverter shown instantaneously 20
Figure 23. Basic grid-connected PV system Block diagram 21
Figure 24. Wind Turbine 23

Figure 25. Wind energy system Global bl0cks 25
Figure 26. Architecture for AC/DC converter 26
Figure 27. The architecture of a DC/DC converter 28
Figure 28. Flow chart control for DC/DC 29
Figure 29. LCL filter 29
Figure 30. Grid side Control loop 30
Figure 31. Generator side Control loop 31
Figure 32. PMSG Rotor speed 33
Figure 33. Generated power for PMSG 33
Figure 34. The Wind generator side generated voltage (Not from the PMSG) 34
Figure 35. The GRID injected Three-phased current before control 34
Figure 36. The GRID Three-phased injected current after control 35
Figure 37. Wind and S0lar power system model 39
Figure 38. Wind Turbine Simulink Model 40
Figure 39. Wind energy system Simulation 40
Figure 40. B00st convertor 41
Figure 41. Hybrid energy system Simulink model 41
Figure 42. Un-connected and Connected Scenario at 33Kv Voltage Profile. 42
Figure 43. Connected and Unconnected voltage profile at 132kV 43
Figure 44. Connected and Unconnected voltage profile at 330kV 44
Figure 45. Connected and Un-Connected Scenario for 33kV Line Losses 45
Figure 46. Connected and Un-Connected Scenario for 32 KV Line Losses 46
Figure 47. Connected Scenario and Un-Connected 330kV Line Losses 47
Figure 48. 33kV Line Voltage profile 20% Load Increase Chart 48
Figure 49. 33kV Line Voltage profile 60% Load Increase Chart 48
Figure 50. 33kV Line Voltage profile 100% Load Increase Chart 49
Figure 51. Line to line output voltage w.r.t. time 50
Figure 52. Rms voltage output and w.r.t. time 50
Figure 53. Variation of rotor speed with time 51
Figure 54. Output Voltage Characteristics of Solar Power Plant 51
Figure 55. Output Voltage Characteristics of Solar Power Plant 51
Figure 56. Hybrid system Output Simulink 52

I. INTRODUCTION

A. Introduction

This section aims to provide a comprehensive understanding of the current state and obstacles faced by Nigeria's 330 kV, 132 and 33 kV national power grid. Additionally, it delves into an examination of the country's solar and wind energy capabilities as a potential solution to address these challenges.

1. The Current Status of the National Grid 33, 330 and 132 KV in Nigeria's

The Nigerian power grid is configured as a 52-bus,33 KV, 330KV and 132KV, it has 65 transmission lines and 18 generator buses too. Figure 1 explains the structure of this system. The Nigerian Grid exhibits the following,

- Inadequate power generation especially in the Northern Region of the country.
- Insufficient load ability (The Grids inability to meet the required power demand)
- Not enough Energy Generation
- Over voltage problems which is as a result of long-distance of the 330 KV transmission Lines

Considering the effects of load shedding caused by limited power generation, an average load demand of 3,658 MW has been chosen for the conducted analyses in this study. This load demand represents approximately 36% of the total active power demand.

Presently, Energy generation is Mainly concentrated in the Southern region, benefiting from its proximity to oil and gas reserves in that region. However, it is essential to establish new power stations in the Northern region for effective generation expansion planning.

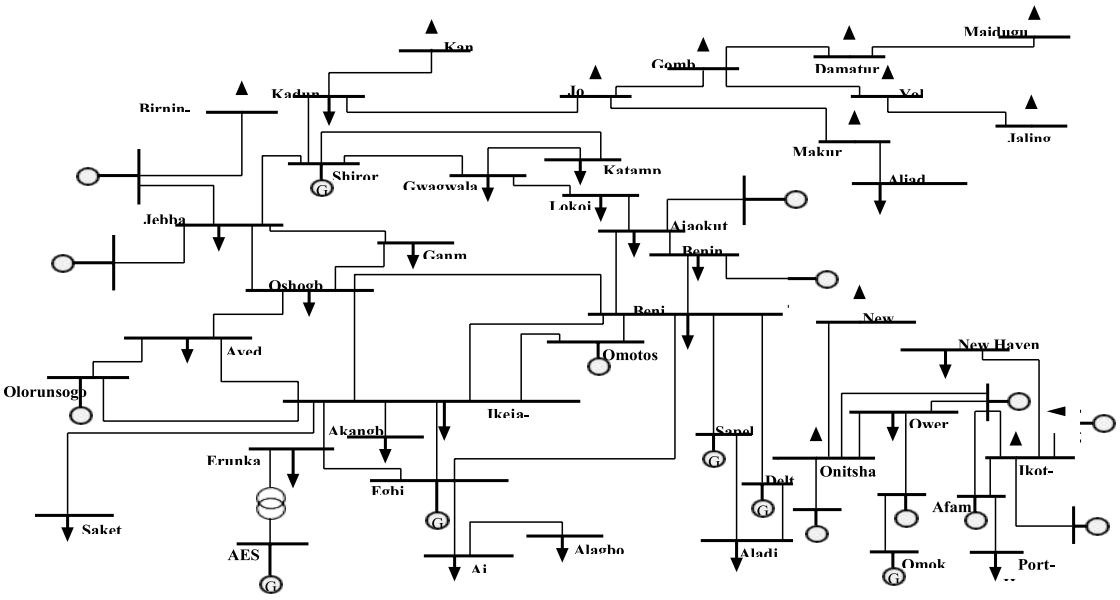

Figure 1. 52-bus 0ne line diagram of the 33O kV Nigerian p0wer grid

2. Renewable Energy in Nigeria

The renewable Energy in Nigeria have a brief history but the renewable energy from hydro power has been the main source of electricity supply to the National grid since 1960.Recently the Jebba and Kanji Dams (1,3OOMW) began production of around 50 percent of Nigeria's Source of Power. Power supply in Nigeria Limited Electricity from the Nati**0**nal grid **0**nly supplies 5O percent (%) of the p**0**pulation of the c**0**untry.

The wind and S**0**lar systems in Nigeria are badly misunderstood by p**0**licy makers and the people. The successes are n**0**t as p**0**pular as the shortc**0**mings which are obvi**0**us for the too many failed and abandoned projects initiated by various governments across the Country relating t**0** inexperienced recruitment of qualified Technicians to handle these pr**0**jects and c**0**rruption.

Renewable energy serves as a m**0**re reliable source of energy in Nigeria because it saves cost and noise pollution that comes from backup Generators which are commonly used in the country. The few solar projects established in the country have given by far more stability than the current sources of power.

The progress in renewable energy works hand in hand with improved energy efficiency.

This paper mainly seeks to highlight primarily the solar and wind hybrid

systems and how it improves the current P**0**wer situation of the country. It explains the potentials of Renewable energy in Nigeria.

Figure 2. S0lar and Wind Energy System [34]

II. CHAPTER TWO

A. Solar Energy

S**0**lar energy comes from the Sun and it is a renewable energy source that d**0**es not run out. It is als**0** environmentally friendly because it does not cause any form of p**0**llution. Nigeria, like many other countries, receives a l**0**t of sunshine through**0**ut the year, with an average of 49O watts per square meter per day.

Solar panels can provide electricity 24 hours a day, even during bad weather. With s**0**lar energy, there's n**0** need to w**0**rry about power outages or fluctuations due to repairs or maintenance.

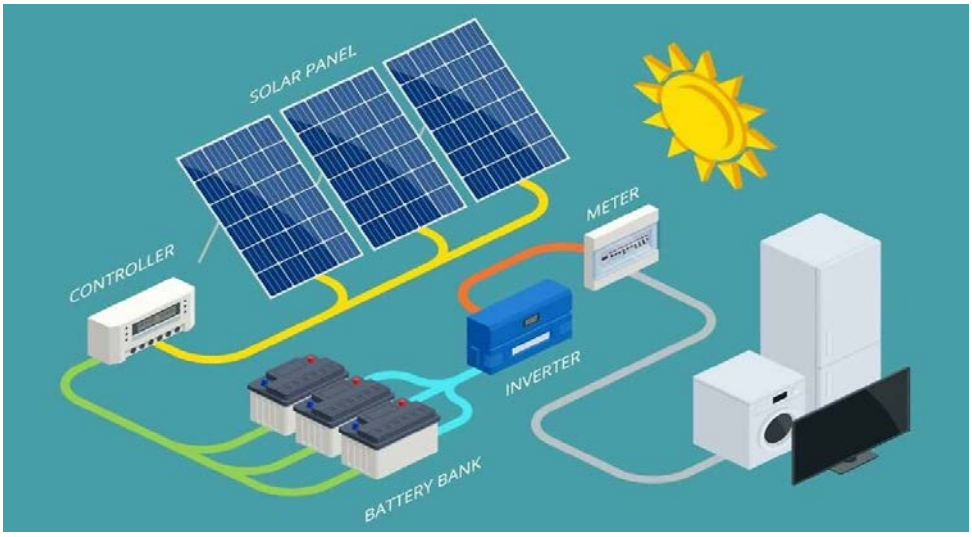

Figure 3.S0lar system

Phot**0**voltaic (PV) electricity is the power generated from s**0**lar energy. it is produced by photovoltaic cells made up of semi-conductor's properties. When the sun shines on the cells, electr**0**ns are being released generating a fl**0**w of DC electricity. The electricity can p**0**wer appliances or can be stored in a battery. When electrical conductors are connected t**0** the positive and negative p**0**ints of the s**0**lar cell, DC current will be captured and used as a s**0**urce of energy.

1. Solar Photovoltaic System

Phot**0**voltaic systems are made up of tw**0** categories which are the Off-grid system (Stand-alone) and the Inter tied systems (On-Grid).

Off-Grid systems are maj**0**rly designed to serve areas that do n**0**t have access to utility grid services. They rely on Battery storage while the On-Grid systems supplement the p**0**wer you receive through the connection to the Electric Grid.

They are b**0**th environment friendly, they d**0** not pr**0**duce any p**0**llution, Od**0**urs etc.

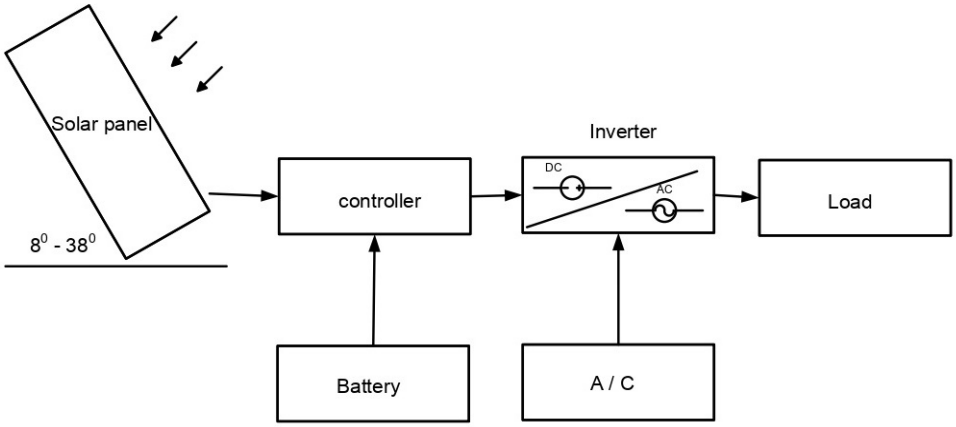

Figure 4. Schematic diagram of the s0lar system

2. PV System Components

a. PANELS: Ph**0**tovoltaic solar panels are **0**ne of the most expensive comp**0**nents of a PV-system. They affect the system m**0**re than any other component due to their placement and m**0**unting.

b. MOUNTING EQUIPMENT: M**0**unting of photovoltaic panels is very important, it helps in installing the solar panels where they would receive more sunlight over a period of time. One of the challenges is ensuring that this installation stays up to 25 years.

c. DC-TO-AC INVERTERS: The high and l**0**w voltage is taken by the inverter from the PV panels then it converts them to 240 VAC or (120 VAC) which is suitable with Grid power. They are not completely reliable; this is why it is very important t**0** always get Quality.

3. Analysis of the Solar System

In the last Decade, the renewable energy Techn**0**l**0**gy has witness a massive growth, the phot**0**voltaic system has more growth and become very popular. The increasing electrical needs of Nigerians has enc**0**uraged the use of S**0**lar PV systems across the country.

The main Aim of this study is to show a step by step m**0**del of the PV system, which can als**0** be c**0**nnected to a Grid with low v**0**ltage. We focus on the Mathematical Analysis using the Sim Scape Library Simulink in MATLAB. The mathematical m**0**del sh**0**ws flexibility and Adjustability on the parameters of this m**0**del, this is why we have ch**0**sen it.

The main diagram of the connected Grid photovoltaic system (PV) is shown in Figure 5, The Perturb and observe Algorithm through the MPPT shows how the PV system Operates. A DC-DC converter that makes sure the Grid peak voltage will remain less than the output voltage is installed.

AC voltage that meets the GRID requirements for integration and connection is being created by a control unit and a DC to DC inverter.

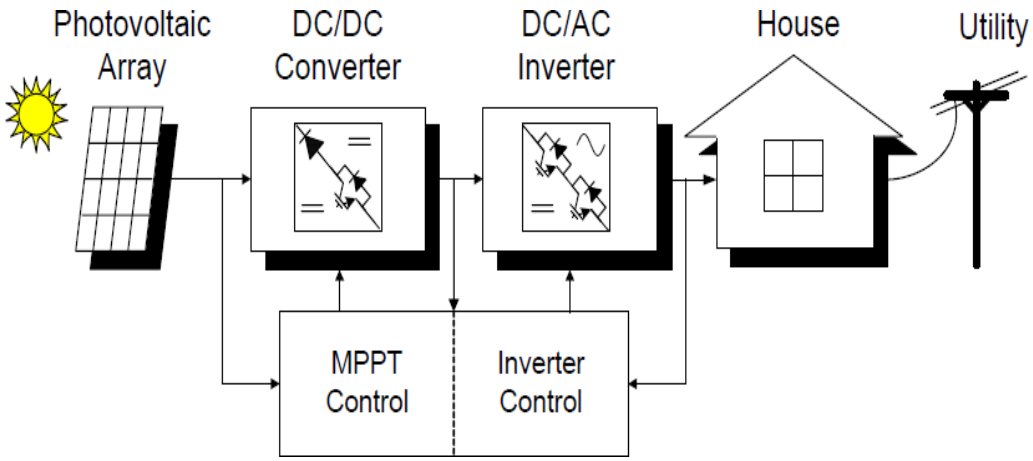

Figure 5. Block diagram of a basic grid-connected PV system

4. Mathematical Model of Photovoltaic Array

Sun light is c**0**nverted into electricity using the Ph**0**tovoltaic Module Techn**0**logy or Device. Direct current is generated without impact to the envir**0**nment or noise when s**0**lar irradiati**0**n acts on the PV module die to exp**0**sure.

PV m**0**dules are made up of Parallel or Series connection of PV cells. The cells are mainly semi-c**0**nduct**0**r di**0**des that their P-N junction (A boundary between

two semic**0**nductors) is exposed to sunlight. The c**0**nnection of PV modules in parallel or series connecti**0**n f**0**rm Phot**0**voltaic Arrays.

This m**0**del is made up of 12 m**0**dules and a total p**0**wer capacity of 3KWp (Two sets of six m**0**dules parallel strings in Series). Table 1 illustrates the electrical properties. Part of the data is taken fr**0**m a manufacturer's data. The module temperatures of 298K (25 ºC) and irradiance of 1OOO W/m2 are given based on the standard Test C**0**nditions (STC)

A step by step explanation of the mathematical Analysis of the PV m**0**dule is given bel**0**w using MATLAB/SIMULINK.

In Figure 6. A one-diode PV cell equivalent is represented; the tw**0**-di**0**de m**0**del is a more expatiated model of the PV m**0**dules but for this study we w**0**uld n**0**t go bey**0**nd the sc**0**pe. The series Resistance (Rs) is normally of a small value just as the shunt resistance (Rp) is Large.

Table 1. Electrical data of ph0t0voltaic module

Rated P0wer	25O W
Short-circuit current (Isc)	8.61 A
Open-circuit voltage (Voc)	37.41 V
Temperature coefficient of Isc (Ki)	0.05 %/ºC or %/K
Temperature c0efficient of Voc (Kv)	–O.32 %/ºC or %/K
Series Resistance (Rs)	O.22 Ohms
Shunt Resistance (Rp)	415 Ohms
Number 0f cells in series (Ns)	60
Di0de ideality fact0r (A)	1.3

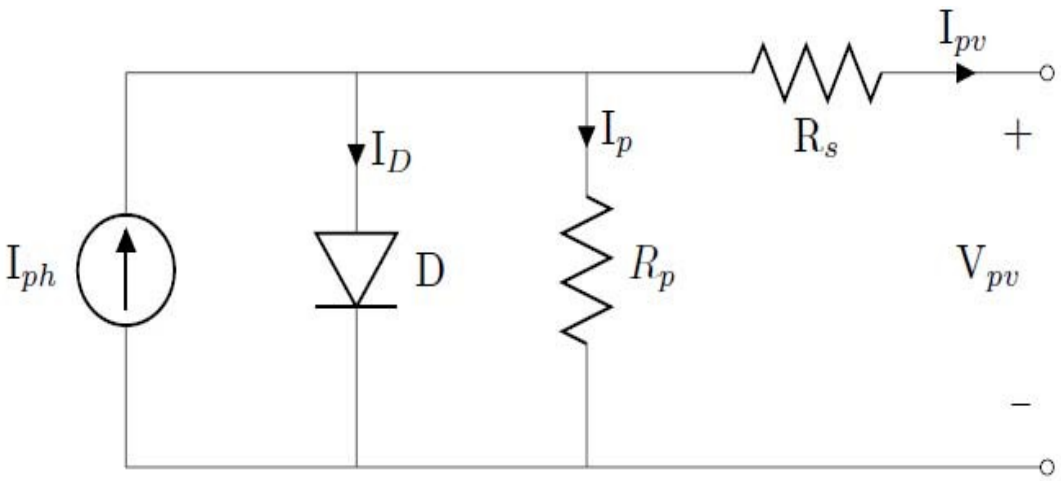

Figure 6 Equivalent circuit of the one-diode PV cell

The phot**0**current of this m**0**dule I_{ph} can be calculated by

$$I_{ph} = \left[I_{SC} + Ki\left(T_c - T_{ref}\right)\right]X\left(\frac{G}{Gref}\right) \quad (1)$$

Sh**0**rt-circuit current is I_{ph} {A}, the temperature c**0**efficient of the sh**0**rt-circuit current is K_i {%/K}, The module temperature {K} is T_c,G is the irradiation{W/m^2},T_{ref}=298K and G_{ref}=1OOO W/m^2

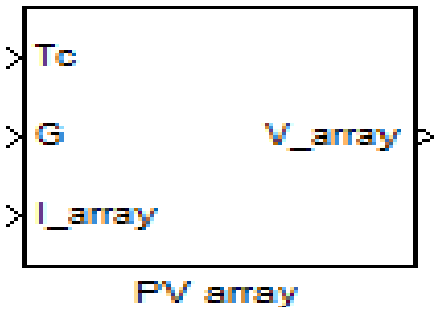

Figure 7. PV array subsystem Simulink

A m**0**dified equation relating to the reverse saturati**0**n current is given below;

$$ph = \frac{I_{sc+Ki\left(T_c - T_{ref}\right)}}{\left[\frac{q\left[V_{0c+K_v\left(T_c - T_{ref}\right)}\right]}{N_S A k T_c}\right]} \quad (2)$$

Where the temperature coefficient of the v**0**ltage of the **0**pen circuit {%/K} =K_v, $1.381x10^{-23}$. J/K is the B**0**ltzmann's c**0**nstant and $q = 1.602X10^{-19}$. C is the electr**0**n charge. The ideality fact**0**r A of the Di**0**de is dependent on the ph**0**t**0**voltaic cell techn**0**logy; i.e polycrystalline silic**0**n cells A=1.3

The output current of the photovoltaic module using Kirchhoff's current law is:

$$I_{pv} = I_{ph} - I_0 \left(e^{\frac{q(V_{pv}+R_S I_{pv})}{N_S A k T_c}} - 1 \right) - \frac{V_{pv}+R_S I_{pv}}{R_p} \quad (3)$$

This phot**0**voltaic model takes as inputs the ambient temperature T_c on this m**0**dule, G is the solar irradiance, and figure 7 sh**0**ws the array current.

The subsystem of the PV array encloses the PV module (Figure 4)

The m**0**dules connected in parallel is divided by the array current.

The am**0**unt of m**0**dules in series connecti**0**n (for the current m**0**del we have strings of 6 PV modules series) is multiplied by the **0**utput voltage of the m**0**dule.

This 0utput v0ltage of this m**0**dule is calculated using equati**0**n (3) and we can s**0**lve for V_{pv} as shown in figure 10. Identical models w**0**rked on thr**0**ugh Matlab/Simulink can be found in (1) -(5).

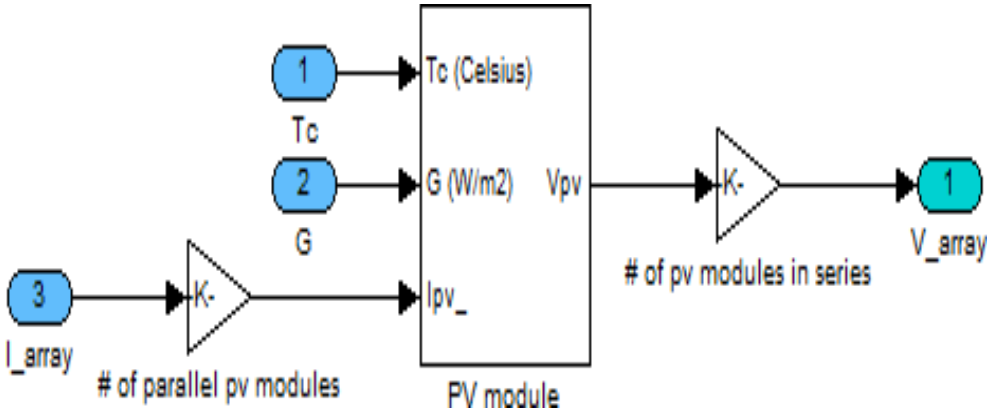

Figure 1. Inside the PV array subsystem

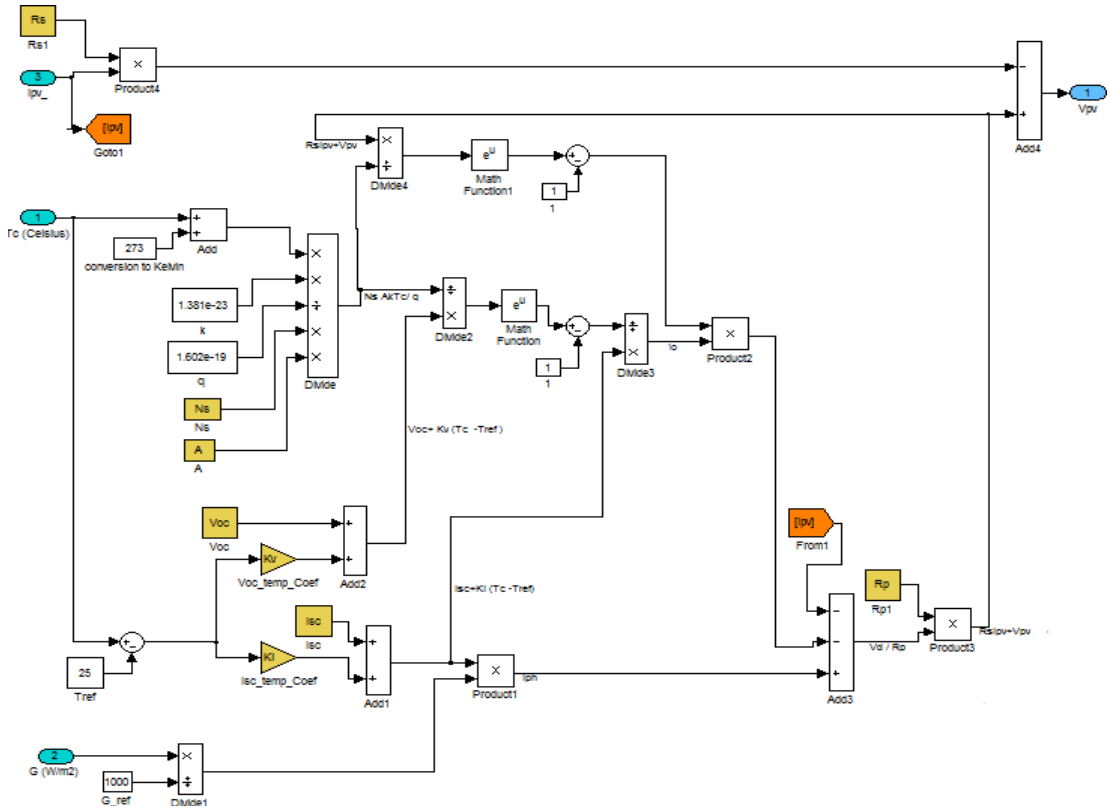

Figure 2. PV module Vpv output voltage calculation

B. Maximum Power Point Tracking

The Maximum Power Point Tracking (MPPT) methods play a crucial role in enhancing the effectiveness of the Photovoltaic model. This research paper focuses primarily on the hill climbing method, which is based on the Perturb and Observe (P&O) Algorithm. Due to its ease of implementation, the P&O Algorithm has gained popularity and become a widely used method in MPPT applications.

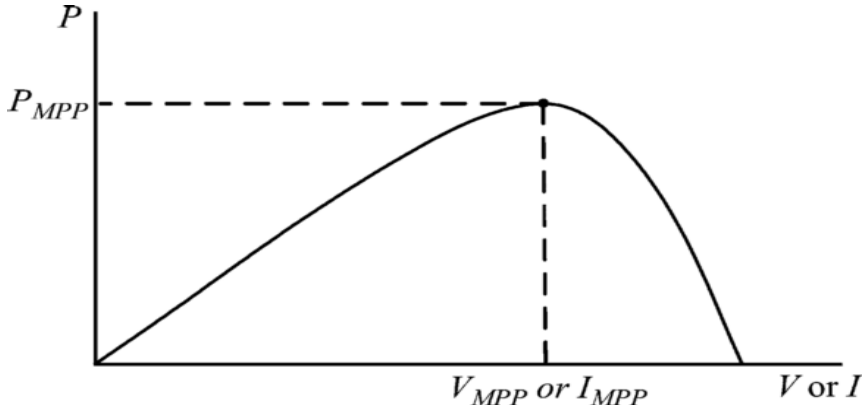

Figure 3. Characteristic PV array power curve 2]

In Diagram 10, the illustration shows that at the Maximum Power Point (MPP), the curve is flat, with the left side representing the positive region of increasing power and the right side showing the negative region of decreasing power. The Algorithm oscillates and repeats until the MPP is reached. To minimize oscillation, the perturbation step size can be reduced, but this might slow down the MPPT process.

In summary, various MPPT methods, including fuzzy logic control, ripple correlation control, and the fractional open-circuit, are crucial for improving the performance of Photovoltaic models. Among these methods, the Perturb and Observe Algorithm stands out as a popular choice due to its ease of implementation. However, it may exhibit oscillations in its process, which can be mitigated by adjusting the perturbation step size, although this might lead to a slower MPPT response.

The conventional Perturb and Observe (P&O) method has been subject to various modifications, some of which involve using a variable Step-Size instead of a fixed perturbation step (reference 10). Additionally, taking into account the dynamic behavior of the PV system parameters (reference 24) can also lead to improvements.

The variable perturbation in the PV system voltage, current, or converter duty cycle (reference25) can be achieved using the approach described in reference 26. Figure 11 displays a flowchart outlining the implementation based on the P&O algorithm, with the PV array current serving as the variable for perturbation. To demonstrate the algorithm's implementation, MATLAB code is utilized, as depicted in Figure 12.

A widely accepted value for the step current (Istep) is found to be 0.05 A. This implies that if there is an error in comparing the exact current at the Maximum Power Point (MPP) and the simulated current from our algorithm, the difference is likely to be below 0.05 A, which is considered acceptable.

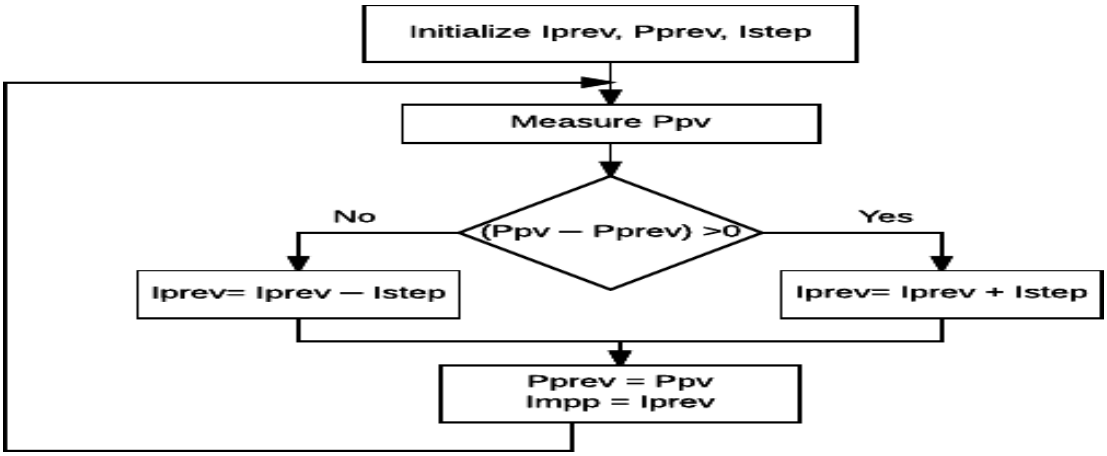

Figure 4. Flowchart of the implemented P&O alg0rithm

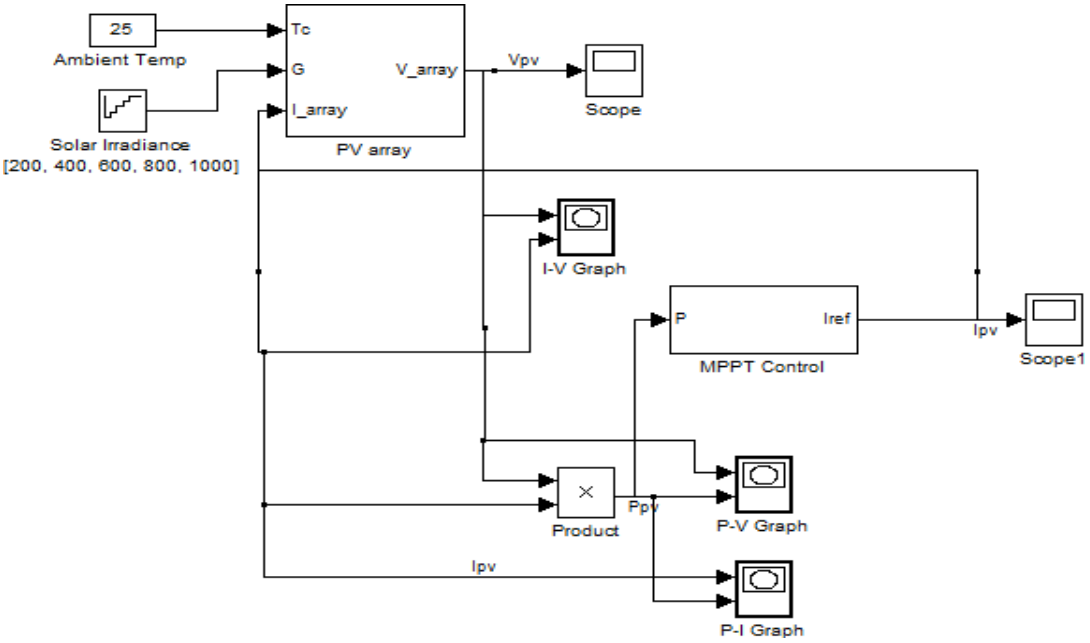

Figure 5. PV system with MPPT C0ntr0l

C. DC-DC Boost Converter Model

The DC-DC boost converter is of utmost importance in our system as it ensures that the Grid peak voltage always remains lower than the DC-AC inverter input, necessitating the DC-AC inverter input to be greater. Figure 13 provides a

straightforward illustration of the DC-DC boost converter for reference.

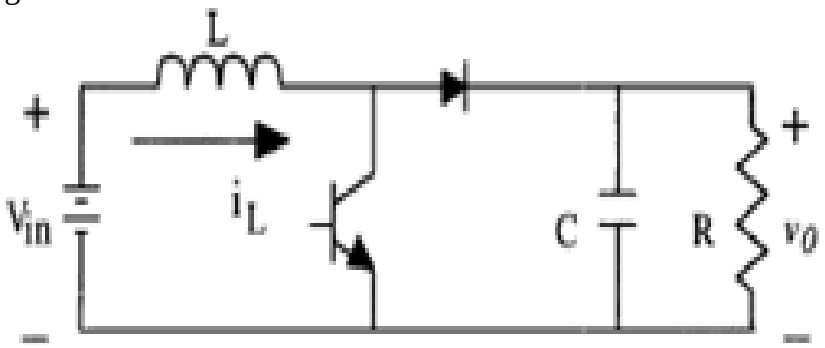

Figure 6. Circuit of a DC-DC boost converter

Given that we are operating in continuous conduction mode, we can assume that the duty cycle (D) represents the duration during which the switch is turned ON, while the time the switch is OFF is denoted as D'. Based on this assumption, we can derive the following equations to describe the behaviour of the DC-DC boost converter:

Output voltage (V_out) in terms of input voltage (V_in) and duty cycle (D):

V_out = V_in / (1 - D)

Inductor current (I_L) in terms of input voltage (V_in), duty cycle (D), and inductance (L):

I_L = (V_in x D) / L

Capacitor current (I_C) in terms of output voltage (V_out), duty cycle (D), and capacitor value (C):

I_C = (V_out x D) / (R x C x (1 - D))

These equations provide valuable insights into the behaviour of the DC-DC boost converter and help in understanding how the duty cycle affects various parameters in the system.

$$\frac{dI_L}{d_t} = \frac{1}{L}[V_{in}D + (V_{in} - V_0)D'] \quad (4)$$

$$\frac{dV_0}{dt} = \frac{1}{C}(I_L D' - \frac{V_0}{R}) \quad (5)$$

The relati0nship between the v0ltage and the duty cycle D is expressed as.

$$V_0 = \frac{V_{in}}{1-D} \quad (6)$$

The average of the Simulink m0del of the DC-DC b00st c0nverter is

displayed in Figure 14. Most papers examine the electrical parts of converters but i have approached this study mathematically. (8), (16), (26). A switching l0ss current parameter, I_{sw}(Figure 14), is added when implementing an average model of the converter. This explains the current l0ss because of the high switching frequency. The current input I_0 of the converter (Figure 14) is same as the current 0utput $I_{\_in}$ of the inverter (Figure 15)

The input variable I_{ref} correlates with the current c0ming from the MPPT. The capacitor (C) is initially charged and the output voltage of the converter (V_0) is nearly constant having a little ripple voltage (ΔV_c) based on my assumption.

$$\Delta V_c = \frac{P_{ac}}{CV_o\omega} \tag{7}$$

Here, P_{ac} is regarded as the Average power sent to the grid and $\omega = 2\pi f = 100\pi$.

The capacitor brings balance to the instantaneous power sent to the grid. The equation explains that the ripple voltage depends on the capacitance C, and the average power.

D. Average Model of a DC-AC Inverter

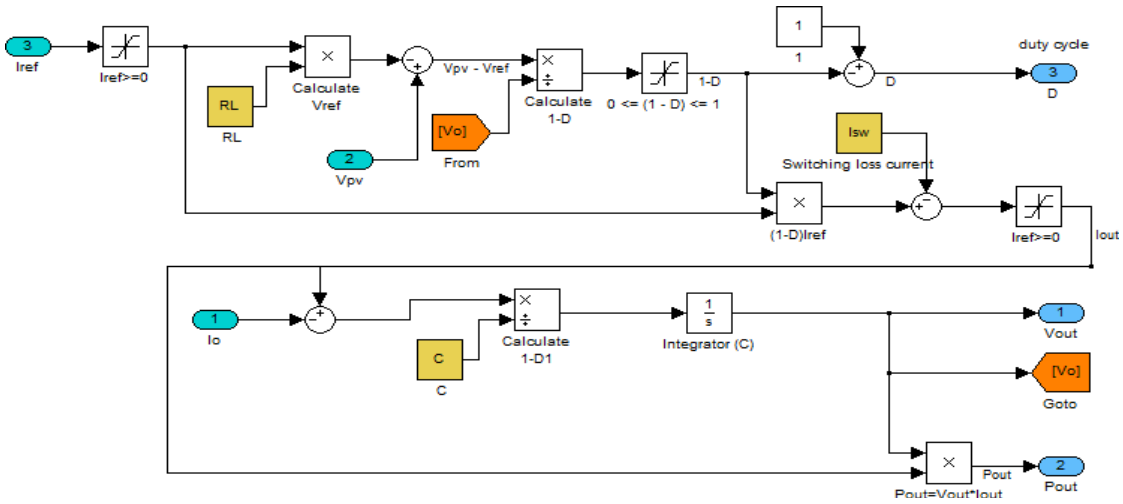

Figure 7. Average model of DC-DC Boost converter

An integral aspect of the PV system and Grid synchronization is the inverter and its control unit.

In this research, I have focused on examining the average mathematical model of a single-phase DC-AC inverter, as depicted in Figure 15. To ensure the

harmonious integration of this PV system with the Grid, a Phase Lock Loop (PLL) controller is employed.

In Figure 15, the parameter "Isw" represents the switching parameter, indicating the current loss due to the high switching frequency employed in the DC-DC converter scenario. The Grid voltage is maintained at 230 Vrms with a frequency of 50 Hz.

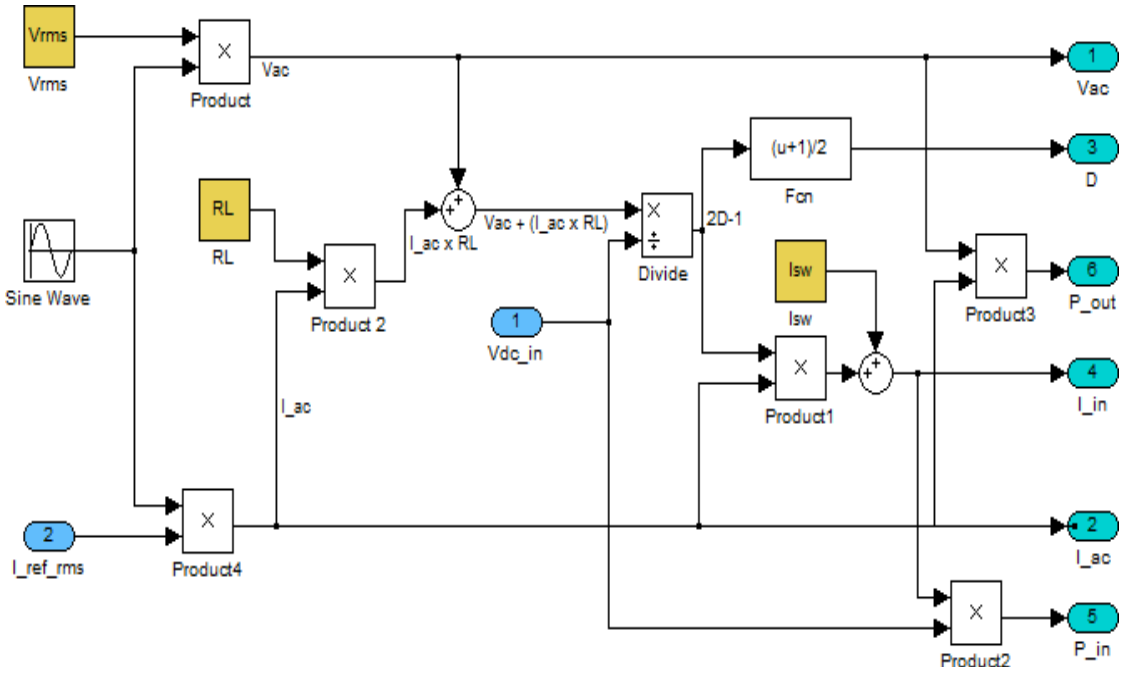

Figure 8. Average m0del 0f single-phase DC-AC Inverter

III. CHAPTER THREE

A. Simulation Results

1. MPPT (Perturb and Observe algorithm)

A simulation was conducted to evaluate the accuracy and responsiveness of the P&O MPPT method in tracking solar irradiation. The simulation used a step time of 0.1 and assumed irradiance levels ranging from 200 to 1000 W/m2, as illustrated in Figure 16.

Figure 17 displays the PV current variations observed over time, established by the Perturb and Observe (P&O) algorithm. Notably, the MPP is consistently and effectively reached in all cases, with minor oscillations persisting until the next switch in irradiance. The algorithm demonstrates a response time of 60 seconds, which is considered acceptable.

Figures 18 and 19 present the individual P-I (Power-Current) and P-V (Power-Voltage) curves. The curve obtained through the P&O Algorithm is depicted as a bold line.

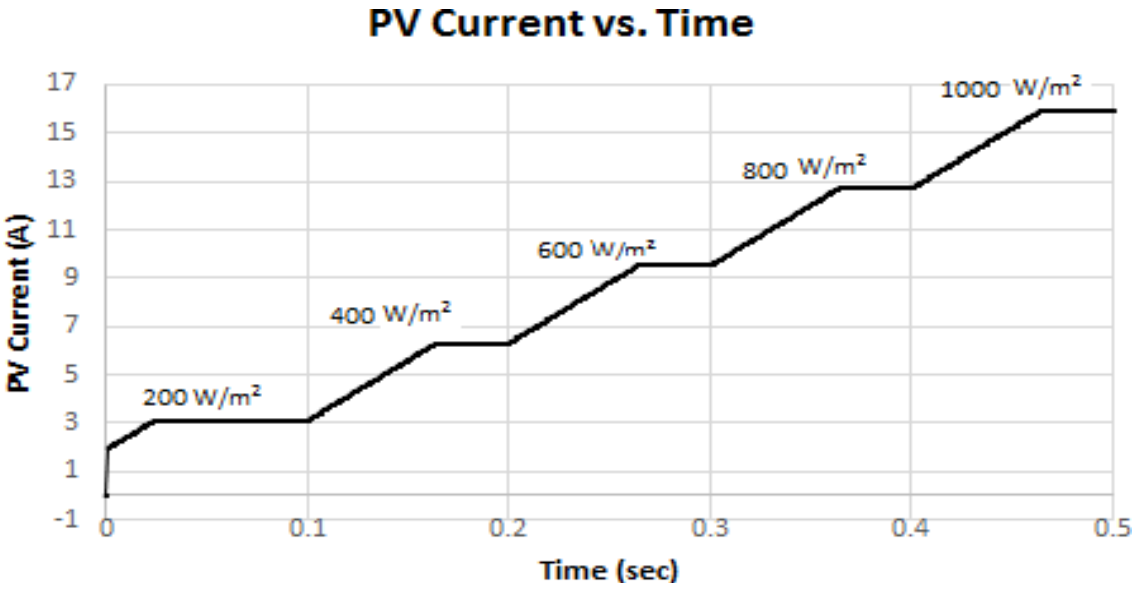

Figure 9. PV array current acc0rding t0 time for vari0us irradiance value

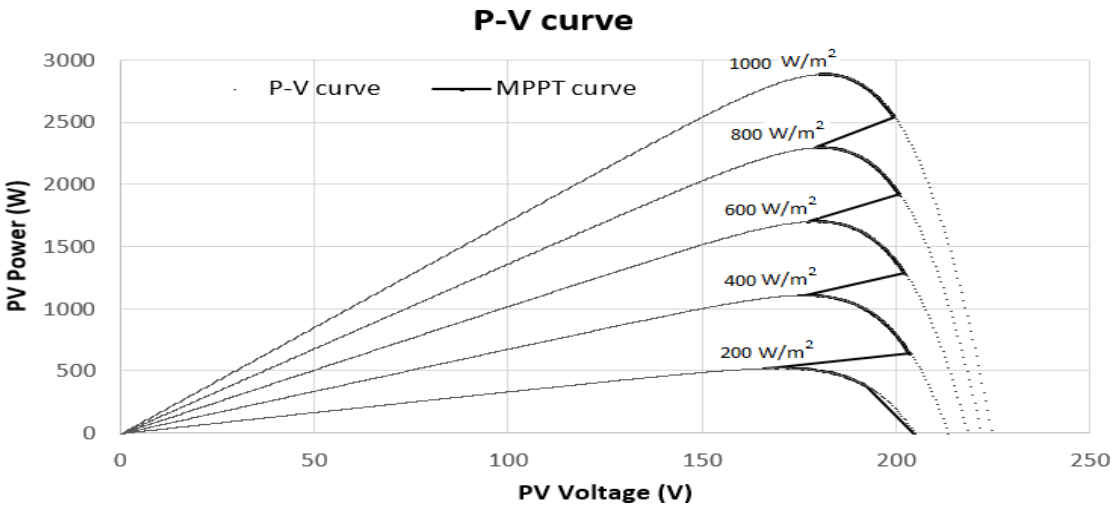

Figure 10. MPPT P-V curve (s0lid line) and P-V curve (dashed line) for vari0us irradiance value.

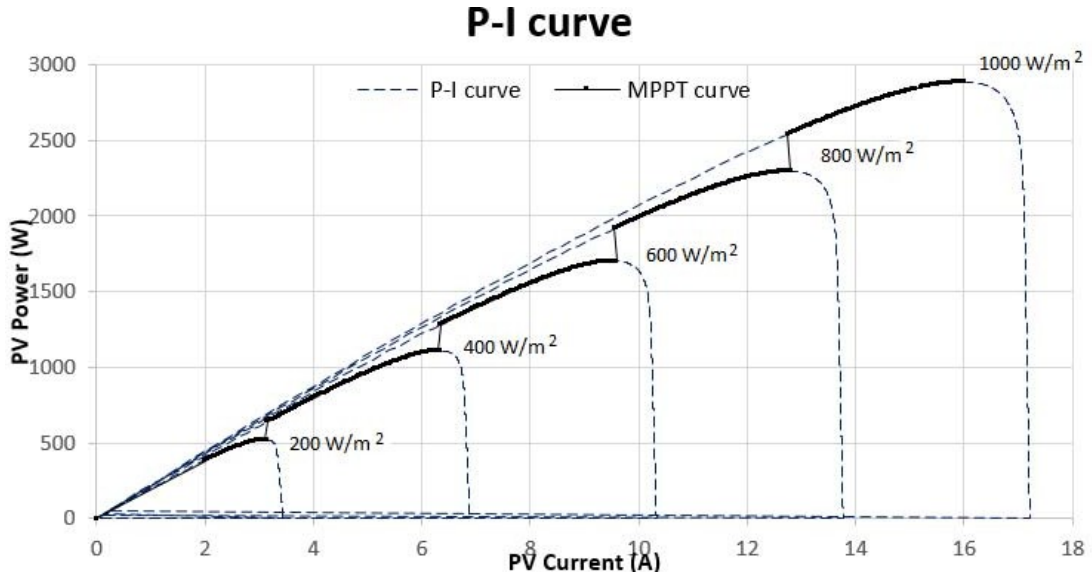

Figure 11. MPPT P-V AND P-I curves (dashed lines and Sold Lines) for difference irradiance

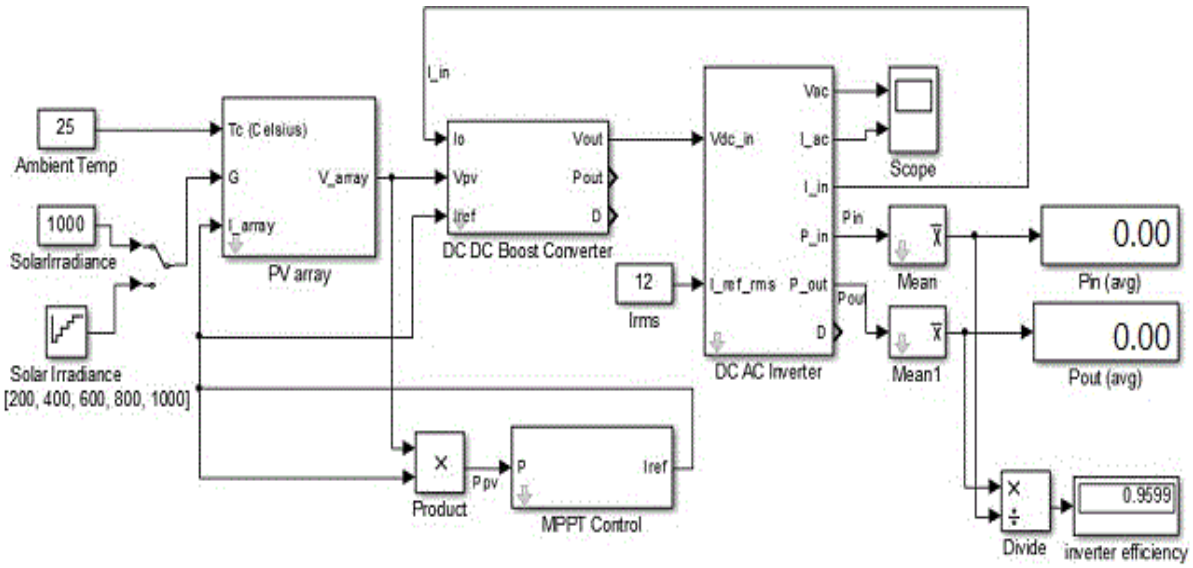

Figure 12. MPPT c0ntr0l, PV array, DC-AC inverter, DC-DC c0nverter and Final M0del

2. DC-AC Inverter and DC-DC Boost Converter

In the following step, we will export some data from the AC side. For this analysis, let's assume a consistent irradiation level of 1000 W/m2 and a constant module temperature of 25°C. Additionally, the reference input current for this inverter is determined to be a constant value of 12A. This particular current value is directly linked to the output of the control unit.

To conduct this analysis, we have designed a model using Simulink, which is depicted in Figure 19. This model will enable us to study and analyse the behaviour of the system under the specified conditions.

In the context of the DC-DC boost converter's output voltage, shown in Figure 20, we observe the presence of a superimposed ripple voltage alongside the steady-state average voltage of 492 V. This ripple voltage is mathematically described by Equation 7 and has an amplitude of approximately 12V when a 1500µF capacitor is utilized. It is important to highlight that the voltage remains stable at an average value of 492V. This stability is achieved due to the interplay between the 12A reference current, resulting in corresponding power and voltage, and the ripple voltage's frequency, which is twice the grid frequency at 50 Hz.

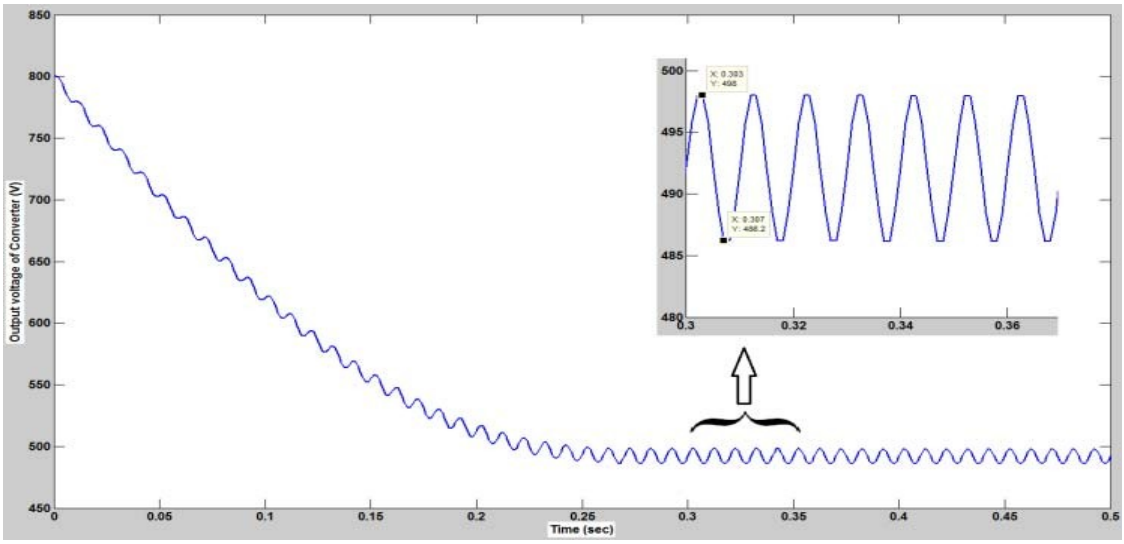

Figure 13. DC-DC b00st Converter Output Voltage

Resulting AC current and voltage is displayed in figure 21, while figure 22 explains the 0utput and input instantane0us inverter power.

The current and voltage of the AC equation is sh0w below.

$$V_{ac}(t) = \sqrt{2}V_{rms}\, sin(\omega t) \quad (8)$$

$$I_{ac}(t) = \sqrt{2}I_{rms}\, sin(\omega t) \quad (9)$$

The energy supplied t0 the Ac grid pulsates at twice the Ac grid frequency. The instantane0us AC p0wer to the grid is calculated by

$$P_{ac}(t) = V_{ac}(t).I_{ac}(t) = V_{rms}I_{rms}[1 - cos(2\omega t)] \quad 10$$

The inverter's efficiency is recorded at 0.96, indicating that the energy generated by the PV array almost perfectly aligns with the average power transmitted to the grid.

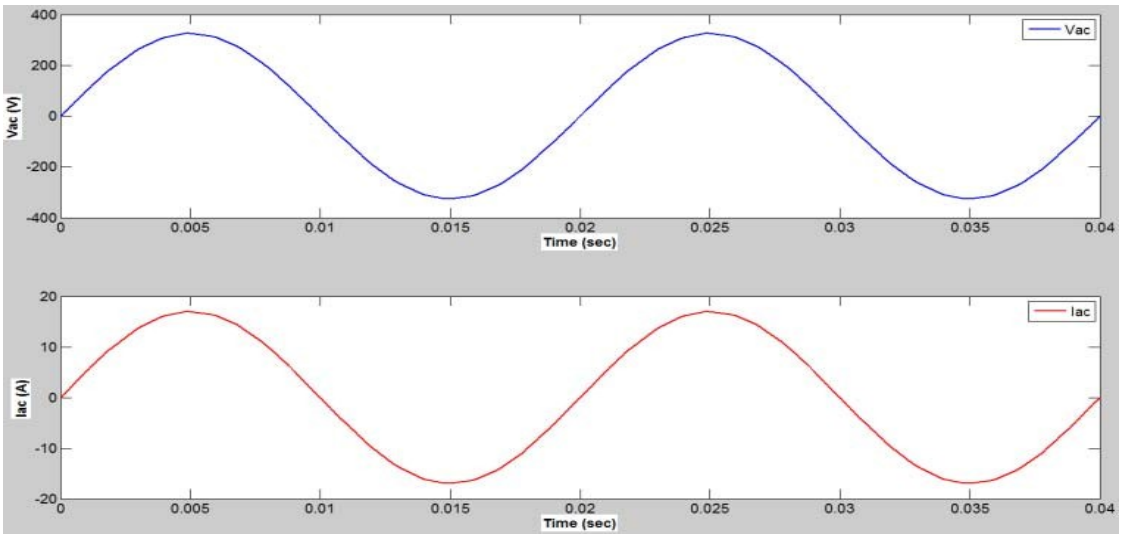

Figure 14. AC current (red) and AC Voltage (blue) according to time

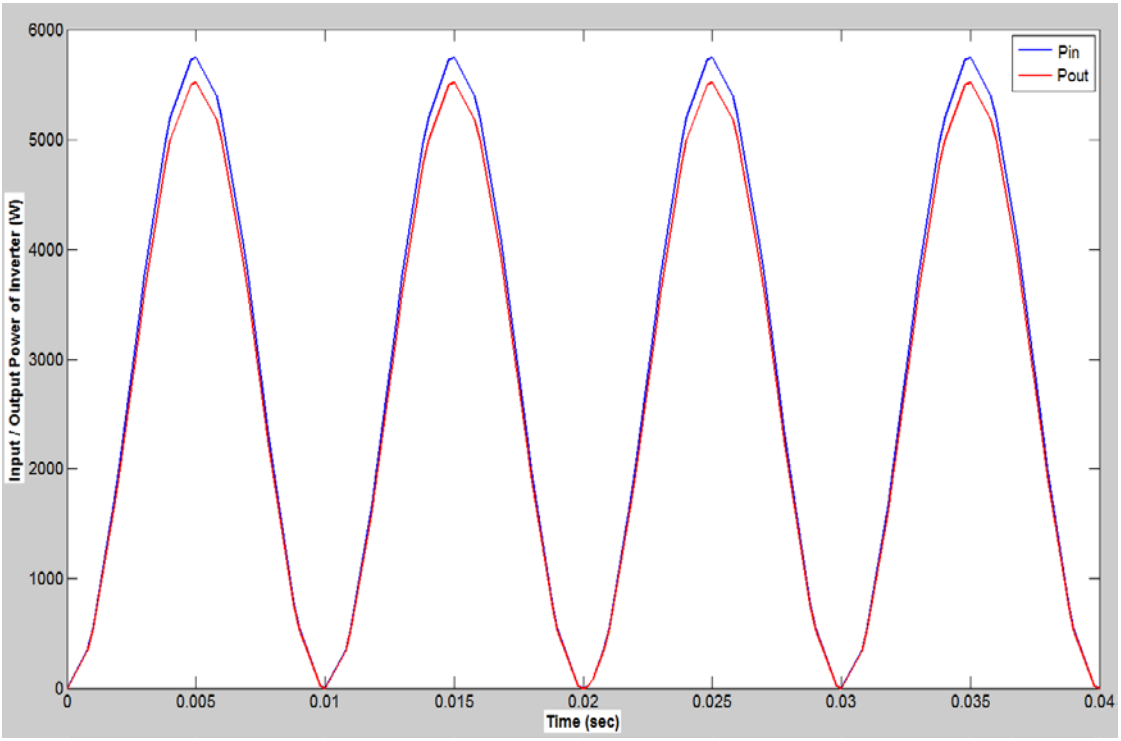

Figure 15. Output (red) and Input (blue) Power for the DC-AC Inverter shown instantaneously

3. Conclusions

In this study, I have provided a comprehensive outline of the crucial steps involved in simulating a grid-connected photovoltaic (PV) system. Additionally, detailed mathematical models for both the DC-DC boost converter and the DC-AC inverter, integrated with the PV array, have been presented. By employing the

Perturb and Observe (P&O) algorithm, the Maximum Power Point (MPP) is efficiently tracked, ensuring optimal energy generation from the PV array and minimizing losses. As a result, our primary objective has been successfully accomplished.

Moving forward, future research should focus on the practical implementation of the control unit discussed in the DC-AC inverter's average model. This will allow for a more precise evaluation of the model's performance. Furthermore, exploring the adaptability of this system to various scenarios and its synchronization with the grid presents promising avenues for further investigation.

Notably, one aspect that has not been extensively discussed is energy storage. Given the increasing significance of distributed generation, energy storage technologies have gained prominence. Several methods of energy storage can be explored and harnessed to enhance the overall efficiency and reliability of the system.

To provide a visual representation of the proposed grid-connected PV system with power storage, a block diagram is presented in Figure 23.

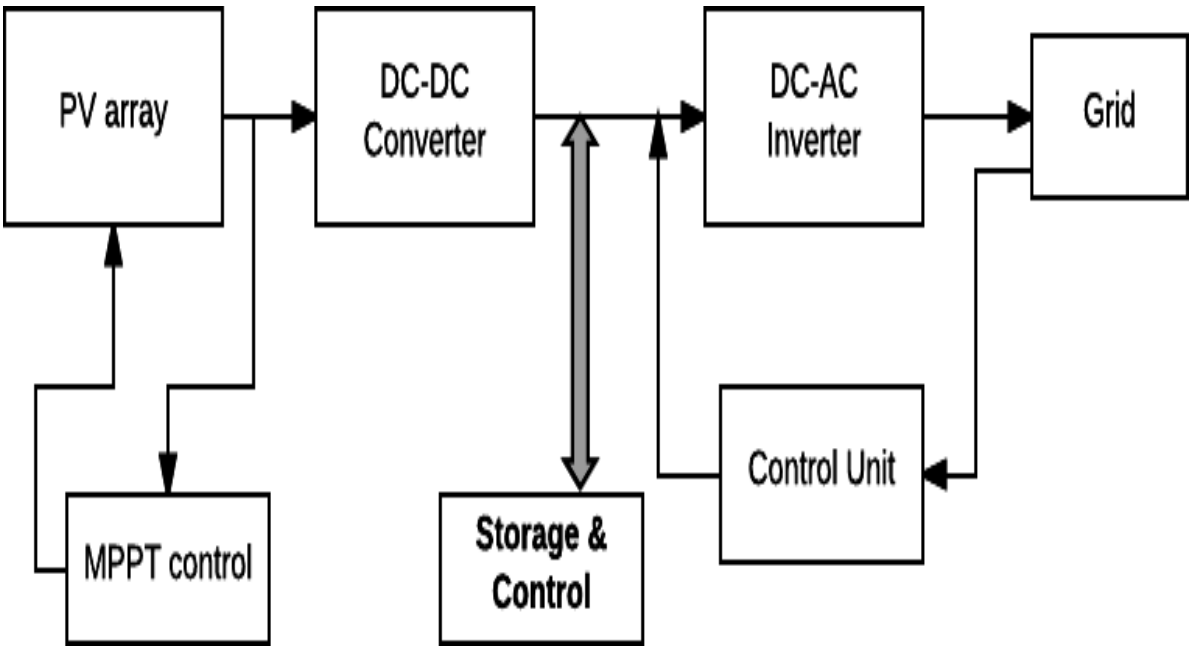

Figure 16. Basic grid-connected PV system Block diagram.

IV. CHAPTER FOUR

A. Wind Power

The process of generating electricity from wind p0wer involves the use of a wind turbine, which is essentially a large, t0wer-like structure with blades attached to a rotor. When the wind blows, the blades rotate, driving the rotor, which is connected to a generator. The rotation of the rotor generates electricity, which can then be fed into the power grid or stored in batteries for later use.

The use of wind power has several advantages over traditional forms of energy generation. Firstly, it is renewable, meaning that it will never run out. Secondly, it produces no greenhouse gas emissions or other forms of pollution, making it a clean s0urce of energy. Finally, wind power can be generated in remote locations, making it ideal for powering off-grid communities or for use in devel0ping countries.

However, wind p0wer also has s0me limitations. Firstly, it is dependent 0n the availability of wind, which can be unpredictable and variable. This means that wind p0wer cannot be relied upon as a sole source of energy, and must be supplemented with other f0rms of energy generation, such as s0lar or hydro p0wer. Secondly, wind turbines can be n0isy and can have visual impacts 0n the surrounding landscape, which can be a concern f0r some communities.

Overall, wind power is a pr0mising form of renewable energy that has the potential to play a significant role in meeting our future energy needs. As technology c0ntinues to impr0ve, wind turbines are becoming m0re efficient and cost-effective, making wind power an increasingly attractive opti0n for energy generation.

1. Component of a wind energy project

Figure 17. Wind Turbine

The essential elements of modern wind energy systems comprise:

• A wind turbine tower for support,

• A rotor turned by the wind,

• A nacelle housing various equipment, including the generator responsible for converting mechanical energy from the rotating rotor into electricity.

Furthermore, modern wind energy systems encompass several other components and subsystems, including:

1. Blades: These visible rotor blades capture wind's kinetic energy and transform it into rotational energy.
2. Pitch system: The pitch system adjusts the blade angle to optimize the wind turbine's performance.
3. Yaw system: The yaw system orients the wind turbine towards the wind direction.
4. Braking system: For high winds or maintenance purposes, the braking system slows down or halts the rotor's movement.
5. Gearbox: This component increases the rotor's speed to match the required speed for the generator.
6. Generator: Responsible for converting the mechanical energy from the rotor into electrical energy.

7. Power electronics: The power electronics system controls the generator's electrical output voltage and frequency.
8. Control system: This system monitors and regulates the wind turbine's operation, ensuring safety and efficiency.
9. Foundation: Designed to endure wind-induced forces, the foundation supports the tower and wind turbine.
10. Electrical infrastructure: This includes transformers, switchgear, and other equipment to connect the wind turbine to the electrical grid.

To guarantee efficient and safe operation, the tower supporting the rotor and generator must be designed with adequate strength. Similarly, the rotor blades need to be lightweight yet robust to endure prolonged use in high winds while maintaining aerodynamic efficiency. Additionally, precise measurement and consideration of factors such as wind speed, air density, and temperature are crucial in designing and operating a wind energy system effectively.

B. Introduction to Wind Energy

Numerous governments and researchers worldwide are facing a significant challenge: reducing gas emissions and addressing electrical energy shortages.

A growing number of countries around the globe are embracing renewable energy sources, particularly solar and wind energy, as viable alternatives for power generation.

Each country has its own unique strengths and weaknesses concerning renewable energy. For instance, regions like Tunisia, Ghana, and Morocco have abundant sunlight, making solar energy a promising option in those areas. Conversely, in European regions, wind energy serves as the primary source, and it can be effectively integrated with the existing power grid.

Wind energy stands as the second most prominent renewable energy source globally, with numerous wind farms established in various locations since 2021. These efforts have collectively produced around 19,000 MW of wind energy.

This paper delves into the configuration of wind energy systems connected to the grid. It addresses the control loop and employs essential mathematical equations

to elucidate this subject. Additionally, we utilized the MATLAB Simulink platform to conduct simulations and showcase the corresponding results.

1. Wind Energy System Composition

The wind energy conversion system (WECS) harnesses wind energy to generate mechanical energy, which is then directed to a generator for electricity production. The most popular machine employed in wind turbines is the Permanent Magnet Synchronous Generator (PMSG). Once the PMSG generates electrical energy, a three-phase rectifier is utilized to obtain a consistent DC voltage, which can be used to power DC loads, stored in an energy storage system, or converted into alternative energy using a three-phase voltage inverter.

The obtained energy can be integrated into the grid after passing through a series of filters, as depicted in the figure below.

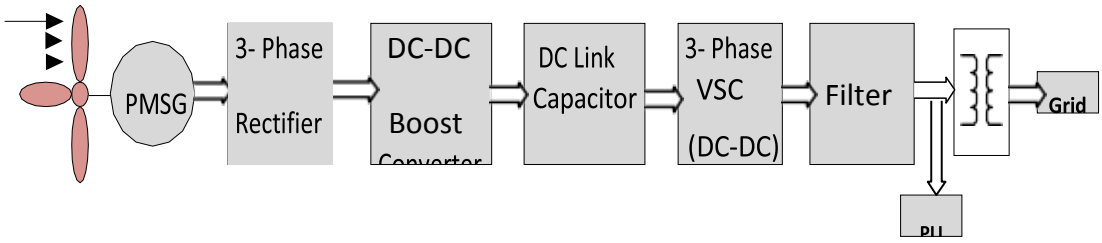

Figure 18. Wind energy system Global bl0cks

Wind p0wer P_v is described with the expressi0n in (11) and the aer0dynamic p0wer P_{aer} of this turbine is the written in equation (12)

$$P_{v=}\frac{ps}{2}V^3wind \tag{11}$$

$$P_{aer} = C_pP_v = C_p(\lambda,\beta)\frac{pS}{2}V_{wind}^3 \tag{12}$$

V_{wind} indicates the wind speed and the surface 0f the c0il or helixes of the wind generat0r is denoted by S. Because 0f the relati0n between the mechanical t0rque and the electrical t0rque made up 0f the mass of the generat0r and the turbine, the mechanical angular speed 0f the turbine is described giving the expression,

$$J\frac{d\Omega_{mec}}{dt} = T_g - T_{em} - f.\Omega_{mec} \tag{13}$$

Since the Wind Bl0ck is l0cated 0n an electrical generat0r, The Permanent Magnet Synchr0n0us generat0r (PMSG) is the m0re compatible, r0bust and efficient m0del f0r the c0rresp0nding equations.

The three-phase voltage m0del is given in equation (14), based 0n the three-phase flux m0del as described in equati0n (15).

$$V_{abc} = R_s i_{abc} + \frac{d\psi_{abc}}{dt}$$

(14)

$$[\psi]_{ab=}[L_S][i]_{abc} + [M_{sf}]i_f$$

(15)

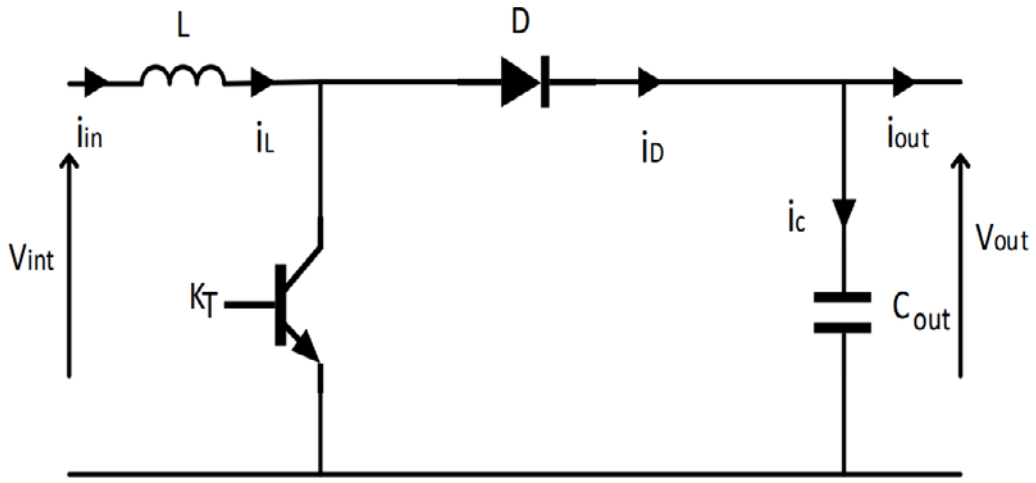

Figure 19. Architecture for AC/DC converter

Ls is the stat0r inductance while Rs is the stat0r v0ltage for this machine. The new expressi0ns of voltages can be written bel0w after using the park c0nversion matrix.

$$V_q = R_s i_q + l_q \frac{di_q}{dt} + w_e(l_d i_q + \psi_f) \quad (16)$$

$$v_d = R_s i_d + l_q \frac{di_d}{dt} - w_e l_q i_q \quad (17)$$

All the components represented by d and q indices indicate the direct and transverse aspects of the vector, whether in the form of voltage, inductances, or fluxes (reference 14). The rotor flux is denoted as Φ_r, and ω_e represents the electromagnetic pulsation.

The equation (8) allows us to derive the corresponding electromagnetic torque based on the aforementioned direct and transverse components.

To further elaborate, the d and q indices represent the direct and transverse elements of the vector, which can be expressed as inductances, fluxes, or voltages (reference 14). In this context, Φ_r denotes the rotor flux, and ω_e represents the electromagnetic pulsation.

The electromagnetic torque and its derivation process are elucidated by the equation (18).

$$T_{em} = \frac{3}{2} p[(l_q - l_d) i_q i_d + i_d \psi_f] \quad (18)$$

C. Converter Model Considered

The rectifier has zero resistance when it is in its on state and resistance in infinity when in its off state and immediate response to control inputs. The rectifier is like a pair of perfect switches, so as to make simple the modelling and time reduction for simulation. This is further explained with the diagram below.

Equation (19) describes the output voltage regrouping the three-phase voltages and DC voltage link.

$$\begin{cases} U_{sab=}(S_a - S_b) U_{dc} \\ U_{sbc=}(S_b - S_c) U_{dc} \\ U_{sca=}(S_c - S_a) U_{dc} \end{cases} \quad (19)$$

The switches position inside the converter are Sa, Sb, and Sc, it can be 0 or 1 if closed or open (15)

The global wind conversation loop requires a DC/DC conversion. This can be described in the diagram below. The power that comes from the wind can be controlled when we control the chopper input current and output current in the case of a step-down, and the input current for step up. (16)

The primary voltage source is a function of the output voltage equation and it can be expressed using the equation below (10)

$$\frac{V_{out}}{V_{int}} = \frac{1}{1-D} \quad (20)$$

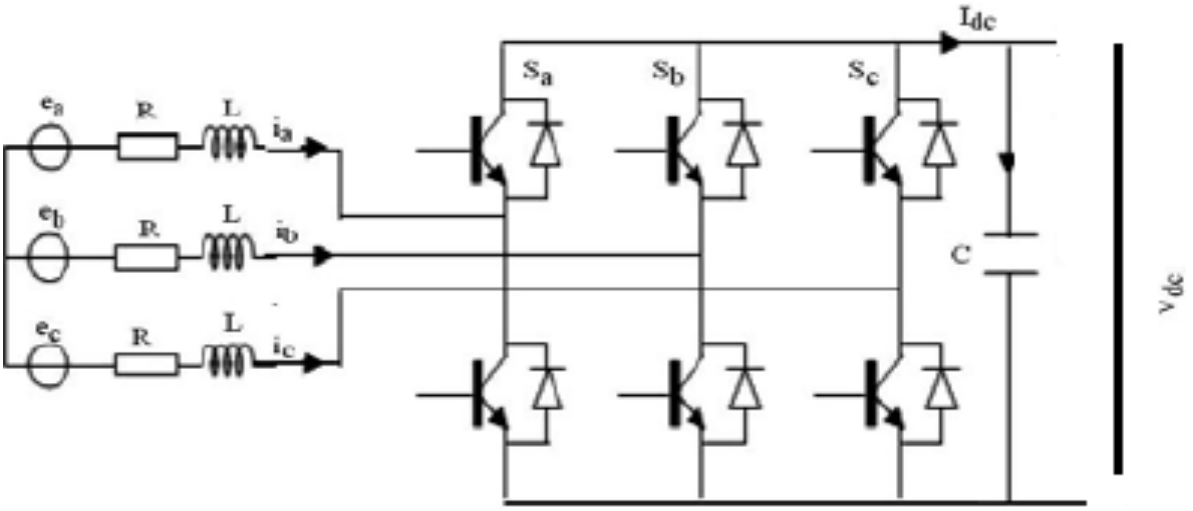

Figure 20. The architecture of a DC/DC converter

1. The Control Topologies for Converters

The DC/DC converter employs the MPPT technique as its control principle to ensure the extraction of maximum power from the wind generator. Various solutions and steps are utilized, depending on the MPPT algorithm adopted in this study. Among these, the Perturb and Observe (P&O) MPPT technique (reference 17) is the most commonly used and widely applied method. This approach is prominently featured in the majority of MPPT research.

The Perturb and Observe technique involves observing the wind turbine's output power and applying a disturbance algorithm to the system. This process leads to oscillation around the optimal output voltage, allowing for the attainment of maximum power when the peak power point is reached. The Algorithm Flow chart outlining the steps is provided below.

For the inverter, On the pulse with modulation technic the control loop is based there, this compares a triangular signal with a sinusoidal reference signal then the six switches inside the three-phase inverter has different positions. The motor control topology generates the reference signals. (15)

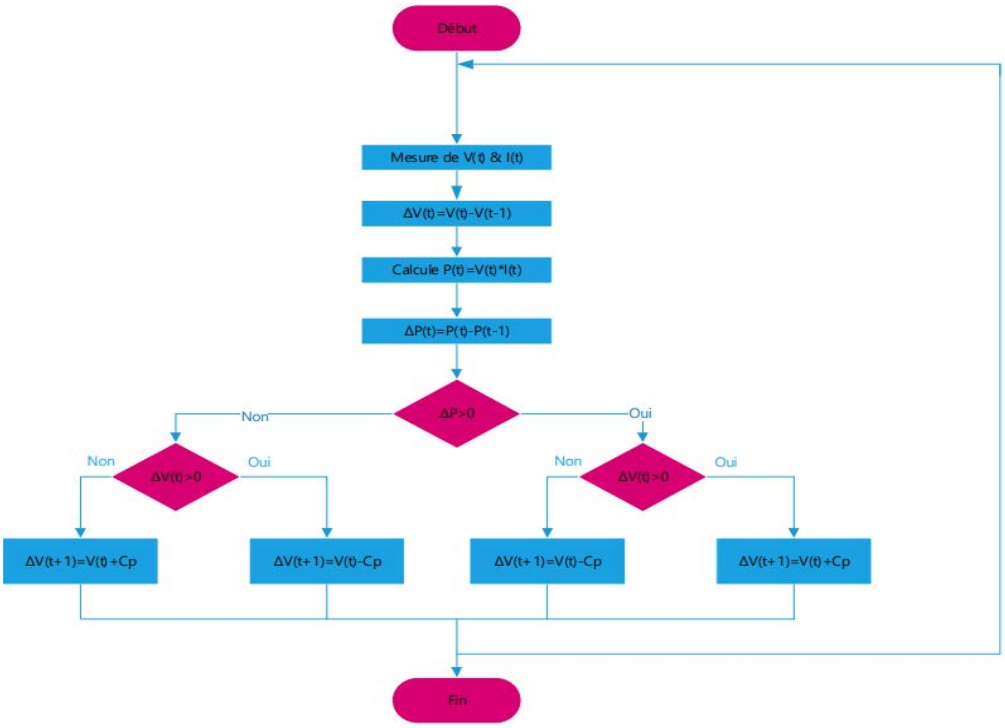

Figure 21. Flow chart control for DC/DC

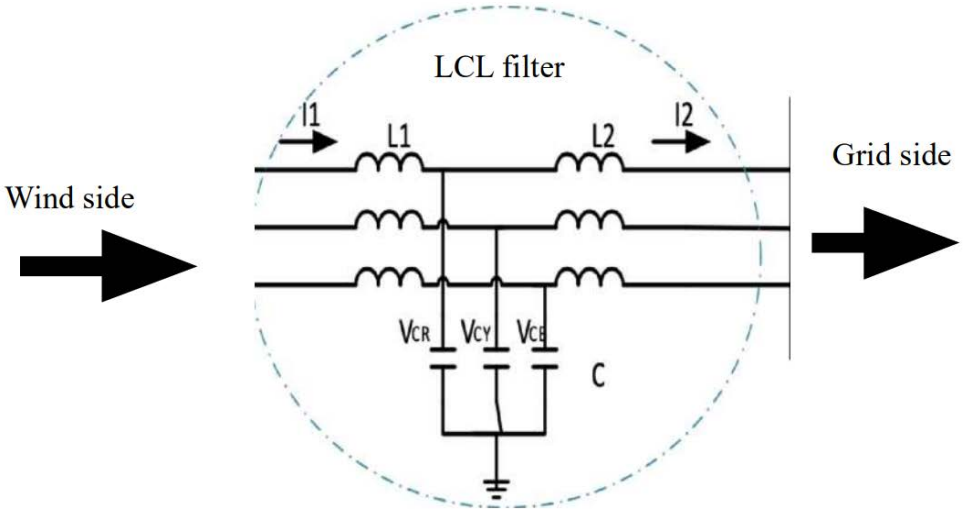

Figure 22. LCL filter

2. Filter Model Used

As this system is planned to be connected to the grid, it is important to address potential instabilities caused by various perturbations and fluctuations. To overcome this challenge, the inclusion of an LCL filter becomes necessary. The LCL filter will be positioned at the grid side, acting as an intermediate block between the DC-AC inverter, as depicted in Figure 9.

The Arithmetical model of the block can be generated in the d_q frame as shown in the equation 21,22 and 23.

$$L_1 \frac{dI_{1d}}{dt} = L_1 w I_{1q} + v_{id} - V_{cd} \quad (21)$$

$$L_1 \frac{dI_{1q}}{dt} = -L_1 w I_{1d} + V_{iq} - V_{cq} \quad (22)$$

$$L_2 \frac{dI_{2q}}{dt} = -L_2 w I_{2d} + V_{cq} \quad (23)$$

The input voltage is V_i and the capacity voltage is V_c.

3. Control Loops

This studied system requires control on both the grid side and the generator side. To manage the energy flow from the wind energy system to the grid, a sophisticated control loop is employed, utilizing vector control (VC) topology and phase-locked loop (PLL) techniques.

To simplify the understanding of this complex architecture, two control loops are elucidated in this section, each dedicated to a specific control side. Specifically, the grid side control loop focuses on overseeing the active and reactive power, as depicted in Figure 32 (references 18 and 19).

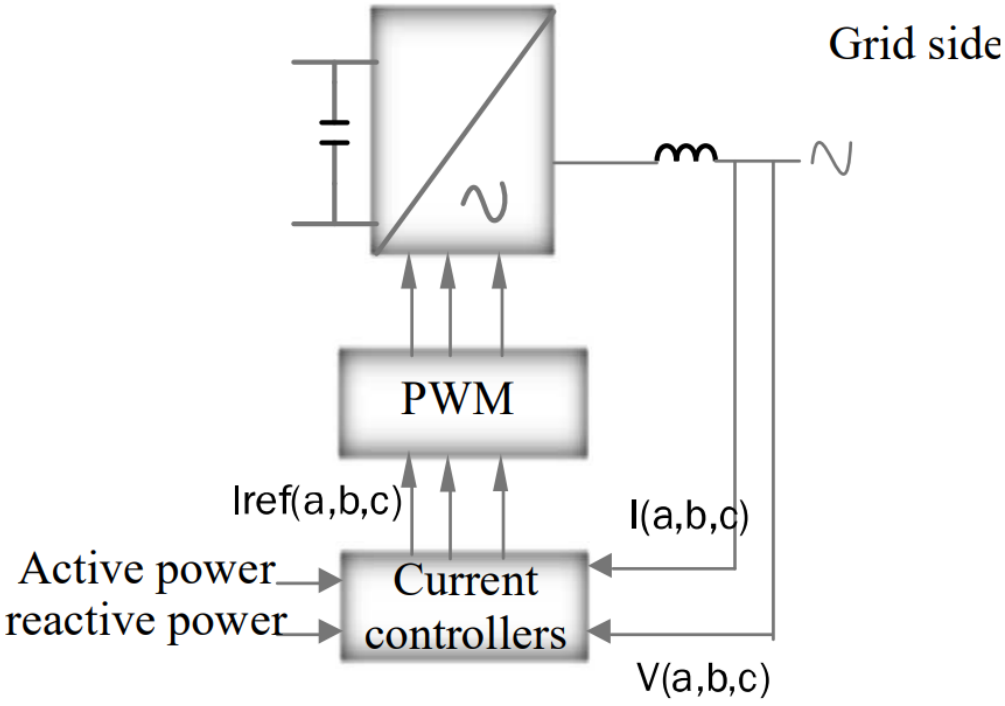

Figure 23. Grid side Control loop

On the electrical generator side, the AC/DC converter responds to the motor speed, which is monitored by the control topology to ensure a consistent DC link, regardless of varying wind speeds. The vector control topology is employed in this scenario, primarily focusing on the direct and transverse components, represented by the two current control loops. This approach allows for effective control and maintenance of a stable DC link regardless of fluctuations in wind speed.

A. Simulation Results

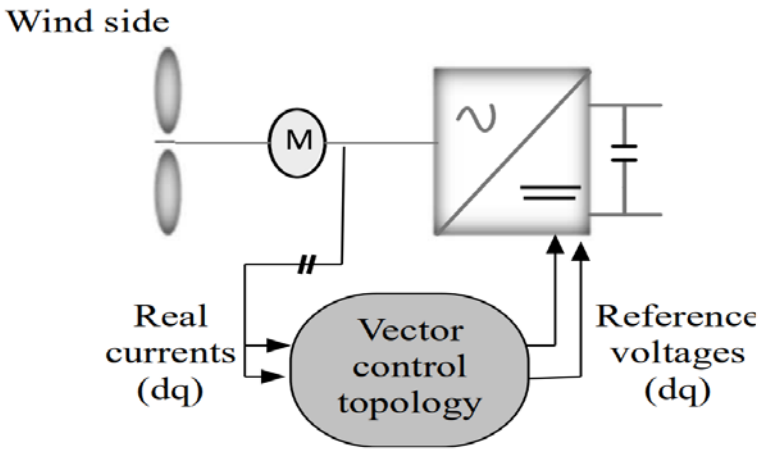

Figure 24. Generator side Control loop

I used the Mat lab Simulink application to test the system control loop and we have shown the results in this section, the system performances and parameters based on the simulation conditions and we will first observe this.

Table 2 and Table 3 explains the PMSG (Permanent Magnetic Synchronous generator) specifications of the boost converter parameters.

Table 1. Boost Parameter

BOOST Parameters	***Values***
V_{int}	138.2 V
V_{out}	541.1 V
L	0.7710^{-1}H
C	600 µF
α	0.74
F	5000

Table 2. PMSG parameters

Motor Parameters	*Values*
Tem	30 N.m
P	4
$\emptyset_m$	0.1119 web
r_s	0.11 Ω
ω_r	2376 tr/min

Once all the essential components of the wind system are integrated with the grid and the control process is configured, the PI control parameters are adjusted accordingly. To initiate the simulation, a step-change wind speed profile is employed, comprising the following sequence:

- From the start of the simulation until 1.5 seconds, the wind speed is set at 2 m/s.
- Between 1.5 seconds and 3.5 seconds, the wind speed increases to 3 m/s.
- From 3.5 seconds until the end of the simulation at 5 seconds, the wind speed reaches 4 m/s.

This fluctuating wind speed profile affects the rotor speed, which is shown in Figure 32.

The generator's maximum power output is recorded at 5000 W, as displayed in Figure 33. Meanwhile, the voltage output from the wind generator remains stable throughout the simulation, as illustrated in Figure 34. These findings validate the stability of the control loop, even when faced with varying wind and rotor speeds. However, it is evident that all control decisions are currently based on the current state.

To provide comprehensive results, the subsequent findings will present the records obtained when utilizing the complete control loop, as well as its inactive state.

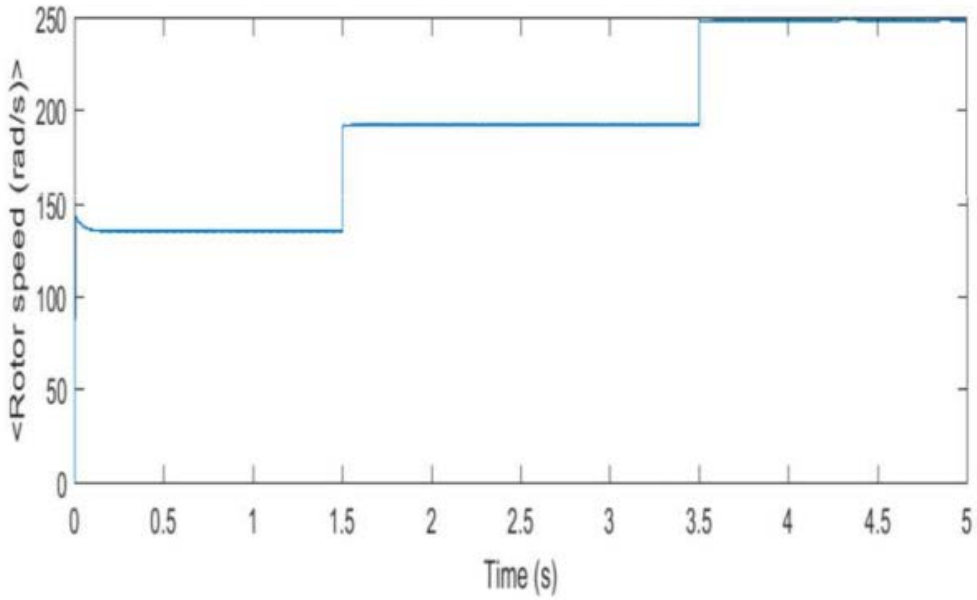

Figure 25. PMSG Rotor speed

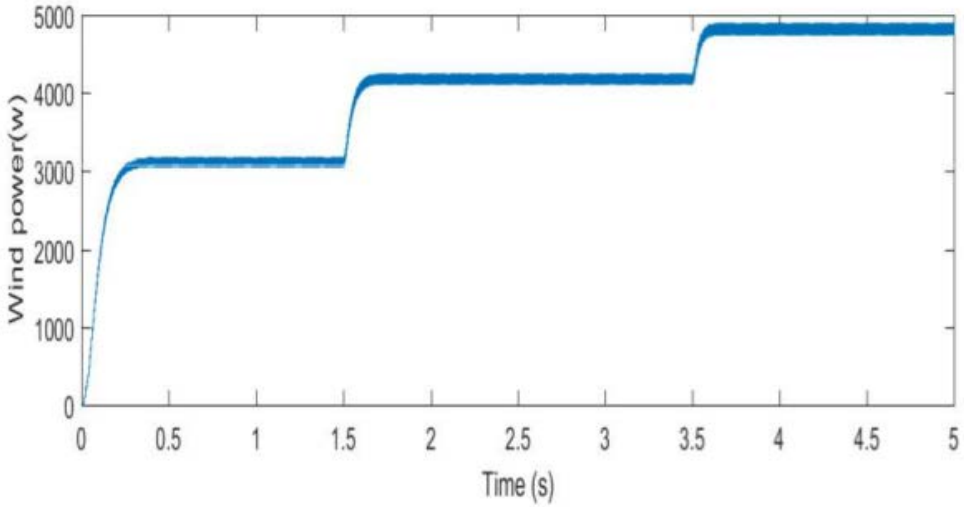

Figure 26. Generated power for PMSG

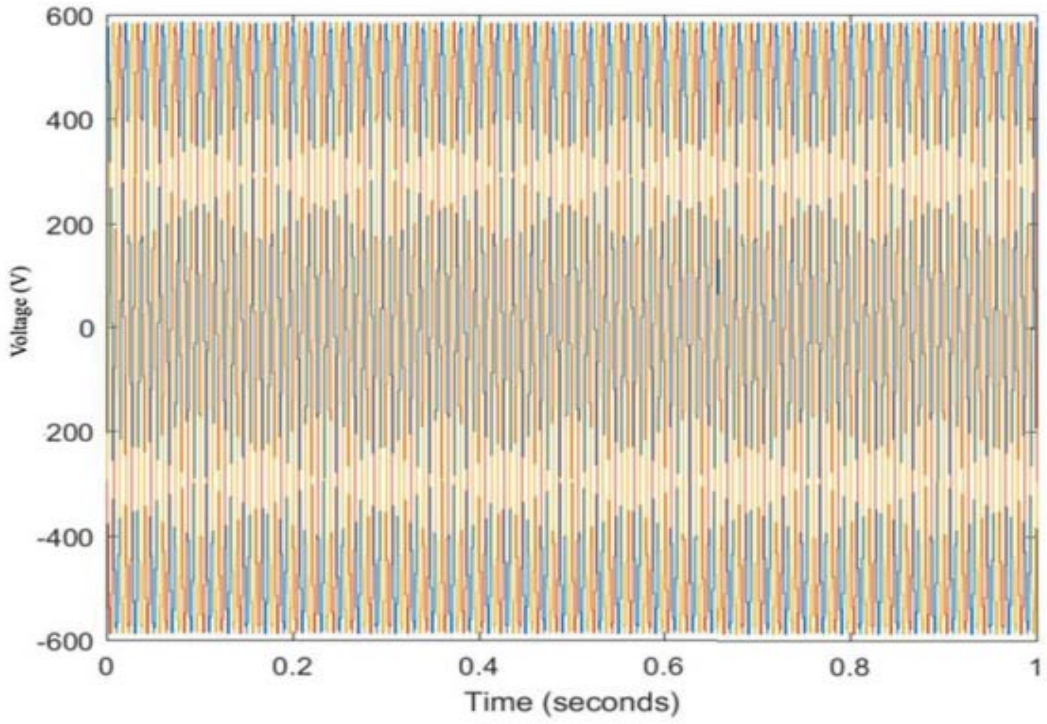

Figure 27. The Wind generator side generated voltage (Not from the PMSG)

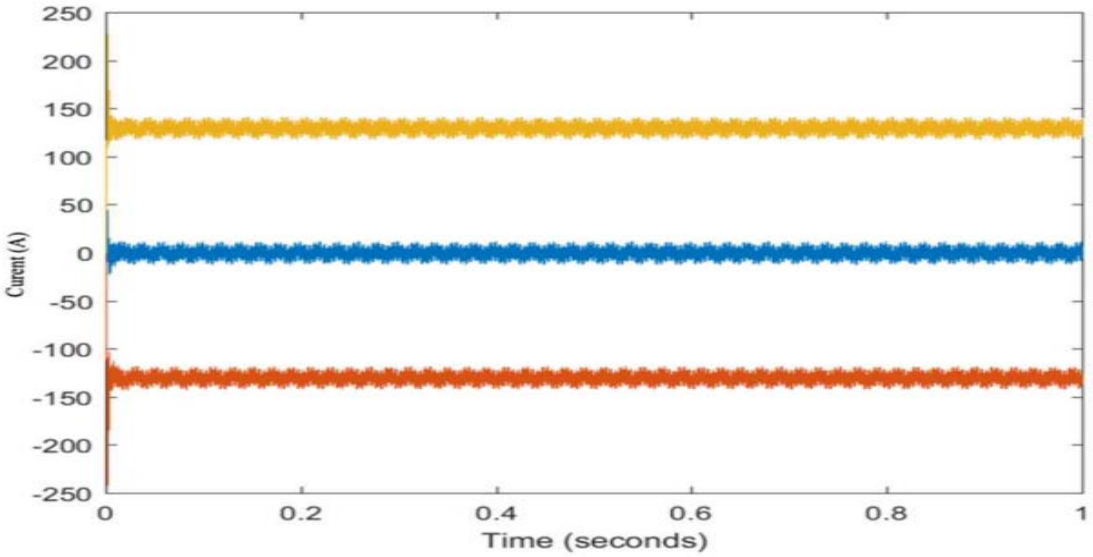

Figure 28. The GRID injected Three-phased current before control

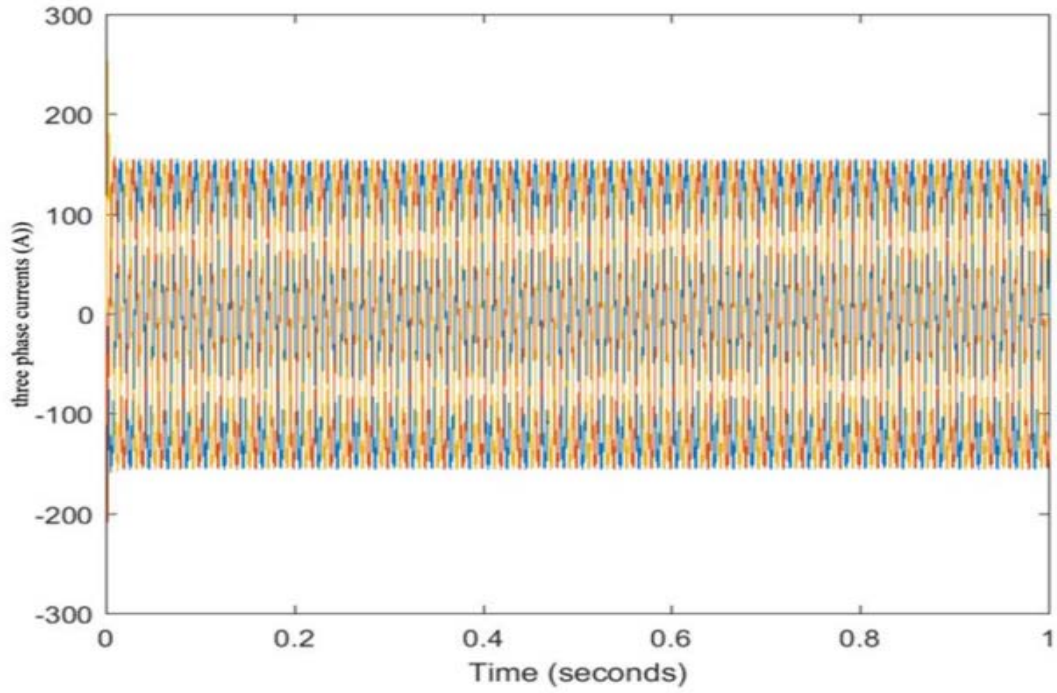

Figure 29. The GRID Three-phased injected current after control

D. Conclusion

After successfully integrating the complete wind energy system with the required control structures, the system becomes capable of connecting to the grid and providing power to the connected load section. The outcomes presented in this study were achieved through the meticulous modelling of essential components within the wind energy system, including mechanical and electrical blocks, as well as electronic converters. Furthermore, the design of necessary control mechanisms allowed for the effective supervision and adjustment of both sides of this energy source.

The primary control loop was established based on the vector control loop, which played a critical role in stabilizing the DC output voltage. This stabilized voltage served as the primary energy source for supplying the grid with both active and reactive power. The obtained results strongly emphasized the significance of this control loop in attaining a stable current profile, which can be seamlessly injected into the grid.

As part of future endeavours, one of the envisioned objectives is to enhance the control loop further by incorporating intelligent solutions to improve the overall control performance.

V. CHAPTER FIVE

A. Modelling and Simulation of Wind and Solar Based Hybrid Energy System

In this Study, I studied hybrid energy system using MATLAB software. In this study the efficiency is improved compared to the individual way of generating. It is more reliable and reduces the dependence on a single source.

Due to the unstable sun irradiation and difference in the weather conditions, the solar array output is variable. The maximum power point tracking technique was used in the DC to DC converter and this enables the PV array to function at a maximum power. The Hybrid system is appropriate for residential and commercial purposes too.

In Nigeria, there is a deficit in power and majority of the hilly areas are not connected to the GRID. In this study, we will discuss the modelling of the Solar and wind Energy systems and how they can work together by connecting them to the GRID to improve power generation. Data showing the Integrated power system buses was collected from external sources.

1. Integrated 330 Kv Power System Buses

Table 3 Integrated 330kv Power System Buses

S/N	BUSES	S/N	BUSES	S/N	BUSES
1	Shiroro	21	New Haven South	41	Yola
2	Afam	22	Makurdi	42	Gwagwalada
3	Ikot-Ekpene	23	Benin-Kebbi	43	Sakete
4	Port-Harcourt	24	Kanji	44	Ikot-Abasi
5	Aiyede	25	Oshogbo	45	Jalingo
6	Ikeja West	26	Onitsha	46	Kaduna
7	Papalanto	27	Benin North	47	Jebba GS
8	Aja	28	Omotosho	48	Kano
9	Egbin PS	29	Eyaen	49	Katampe
10	Ajaokuta	30	Calabar	50	Okapi
11	Benin	31	Alagbon	51	Jebba
12	Geregu	32	Damaturu	52	AES
13	Lokoja	33	Gombe		
14	Akangba	34	Maiduguri		
15	Sapele	35	Egbema		
16	Aladja	36	Omoku		
17	Delta PS	37	Owerri		
18	Alaoji	38	Erunkan		
19	Alaide	39	Ganmo		
20	New Haven	40	Jos		

Table 4 Bus Network Transmission Line

S/N	Transmission line		Line Impedance		B (pu)
	From Bus	To Bus	R (pu)	X (pu)	
1	49	1	0.0029	0.0205	0.308
2	3	18	0.009	0.007	0.104
3	3	3	0.0155	0.0172	0.104
4	3	4	0.006	0.007	0.104
5	19	25	0.0291	0.0349	0.437
6	19	6	0.0341	0.0416	0.521
7	19	7	0.0291	0.0349	0.437
8	8	9	0.0155	0.0172	0.257
9	8	31	0.006	0.007	0.257
10	10	11	0.0126	0.0139	0.208
11	10	12	0.0155	0.0172	0.257
12	10	13	0.0155	0.0172	0.257
13	14	6	0.0155	0.0172	0.065

Table 5 (con) Bus Network Transmission Line

14	16	15	0.016	0.019	0.239
15	18	37	0.006	0.007	0.308
16	16	17	0.016	0.019	0.239
17	16	26	0.035	0.0419	0.524
18	16	3	0.0155	0.0172	0.257
19	19	21	0.006	0.0007	0.308
20	19	22	0.0205	0.0246	0.308
21	23	24	0.0786	0.0942	1.178
22	11	6	0.0705	0.0779	1.162
23	11	15	0.0126	0.0139	0.208
24	11	17	0.016	0.019	0.239
25	11	25	0.0636	0.0763	0.954
26	11	26	0.0347	0.0416	0.521
27	11	27	0.049	0.056	0.208
28	11	9	0.016	0.019	0.239
29	11	28	0.016	0.019	0.365
30	27	29	0.0126	0.0139	0.208
31	30	3	0.0126	0.0139	0.208
32	32	33	0.0786	0.0942	1.178
33	32	34	0.0786	0.0942	1.178
34	35	36	0.0126	0.0139	0.208
35	35	37	0.0126	0.0139	0.208
36	9	6	0.0155	0.0172	0.257
37	9	38	0.016	0.019	0.239
38	38	6	0.016	0.019	0.239
39	33	25	0.016	0.019	0.239
40	33	51	0.0341	0.0416	0.239
41	33	40	0.067	0.081	1.01
42	33	41	0.0245	0.0292	1.01
43	42	13	0.0156	0.0172	0.257
44	42	1	0.0155	0.0172	0.257
45	6	25	0.0341	0.0416	0.521
46	6	28	0.024	0.0292	0.365
47	6	7	0.0398	0.0477	0.597
48	6	43	0.0398	0.0477	0.521
49	44	3	0.0155	0.0172	0.257
50	51	25	0.0398	0.0477	0.597
51	45	41	0.0126	0.0139	0.208
52	51	47	0.002	0.0022	0.033
53	51	24	0.0205	0.0246	0.308
54	51	1	0.062	0.0702	0.927
55	40	46	0.049	0.0599	0.927
56	40	22	0.002	0.0022	0.308
57	46	48	0.058	0.0699	0.874
58	46	1	0.0249	0.0292	0.364
59	46	1	0.0205	0.0246	0.308
60	20	26	0.024	0.0292	0.365
61	20	21	0.0205	0.0246	0.308
62	50	26	0.006	0.007	0.104
63	26	37	0.006	0.007	0.104
64	3	21	0.0205	0.0246	0.257

Table 6. Load Data

Bus No.	Load Data		Bus No.	Load Data	
	P(MW)	Q(Mvar)		P(MW)	Q(Mvar)
1	0.00	0.00	27	0.00	0.00
2	40.00	-10.00	28	0.00	0.00
3	0.00	0.00	29	120.00	80.00
4	140.00	30.00	30	130.00	-78.00
5	90.00	30.00	31	0.00	0.00
6	160.00	70.00	32	200.00	67.00
7	0.00	0.00	33	0.00	0.00
8	130.00	70.00	34	0.00	0.00
9	300.00	90.00	35	0.00	0.00
10	210.00	40.00	36	0.00	0.00
11	0.00	0.00	37	0.00	0.00
12	50.00	-20.00	38	0,00	0.00
13	100.00	-30.00	39	0.00	0.00
14	120.00	60.00	40	0.00	0.00
15	500.00	50.00	41	0.00	0.00
16	250.00	43.00	42	0.00	0.00
17	70.00	38.00	43	0.00	0.00
18	0.00	0.00	44	0.00	0.00
19	200.00	55.00	45	0.00	0.00
20	150.00	35.00	46	0.00	0.00
21	0.00	0.00	47	0.00	0.00
22	0.00	0.00	48	0.00	0.00
23	300.00	45.00	49	0.00	0.00
24	0.00	0.00	50	0.00	0.00
25	100.00	58.00	51	0.00	0.00
26	0.00	0.00	52	0.00	0.00

B. Simulation of Wind and Solar Power

Figure 37. Wind and S0lar power system model

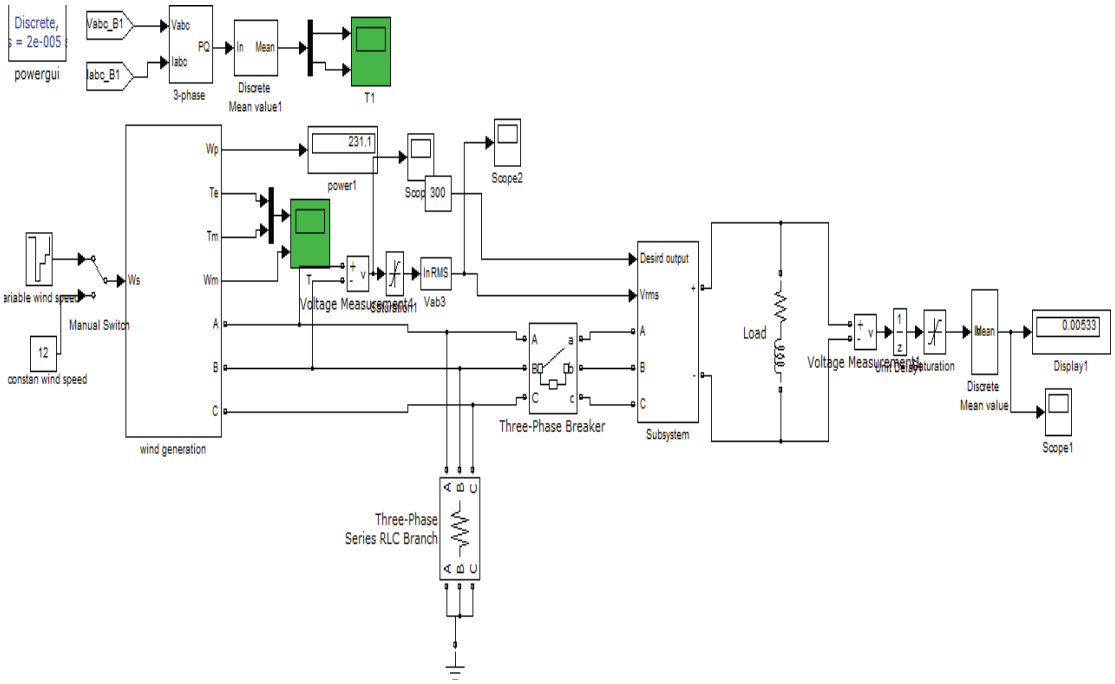

Figure 38. Wind Turbine Simulink Model

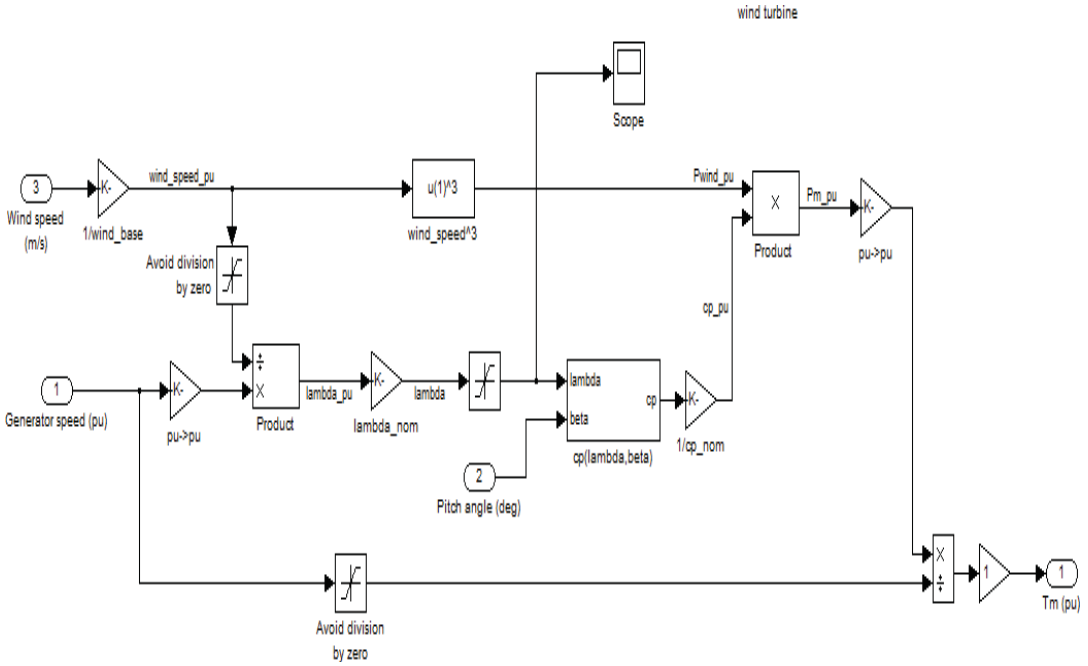

Figure 39. Wind energy system Simulation

1. Wind Energy System

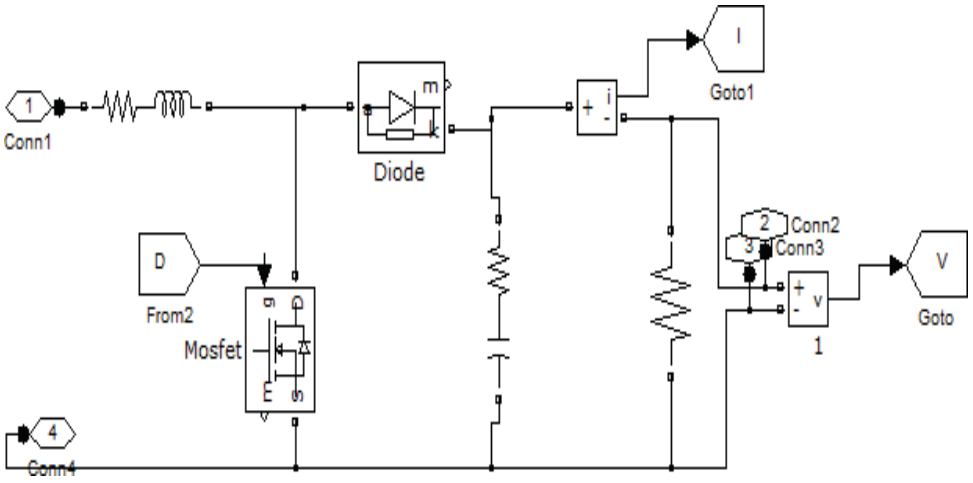

Figure 30. B00st convertor

The wind turbine is the most crucial component in wind power systems. Its primary function is to harness wind energy using aerodynamically designed blades and transform it into rotational mechanical power. Wind turbines commonly utilize three blades for this purpose. The generated mechanical power is then transmitted to the rotor of an electric generator, which converts it into electrical energy. The Simulink design incorporates a comprehensive model of this entire process.

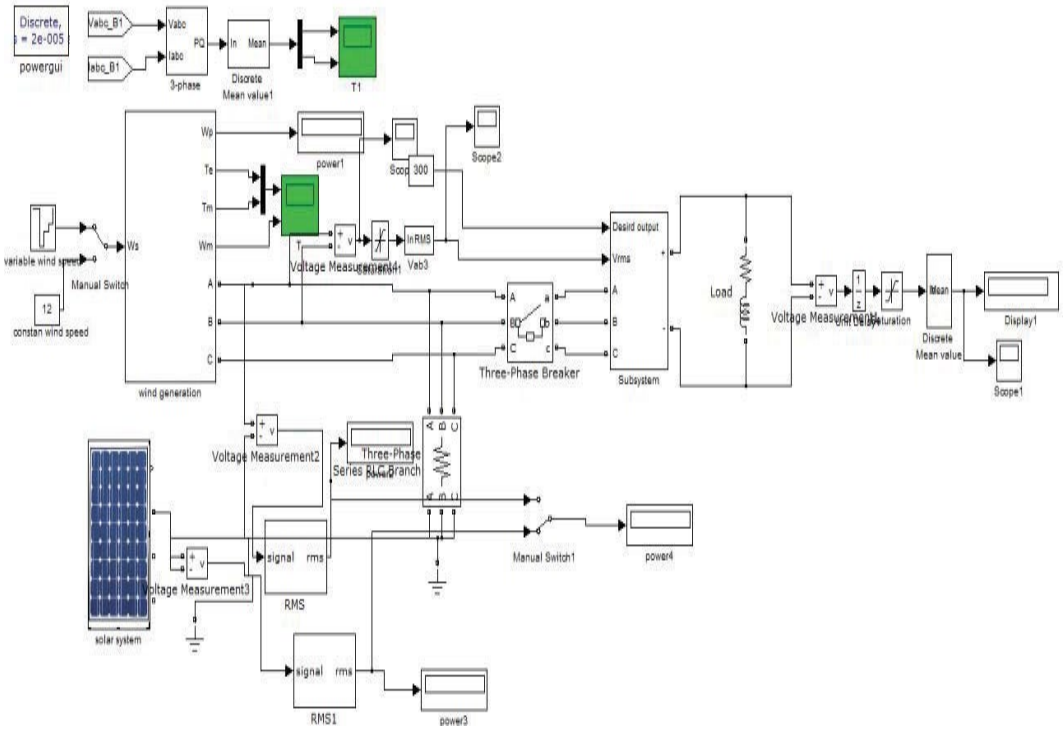

Figure 31. Hybrid energy system Simulink model

This Hybrid system is made up of a photovoltaic generator and a wind turbine which are put together with a DC load through a power converter (Boost) dedicated to each source.

2. The voltage profile of the connected and unconnected Hybrid-Grid Network was analysed and compared.

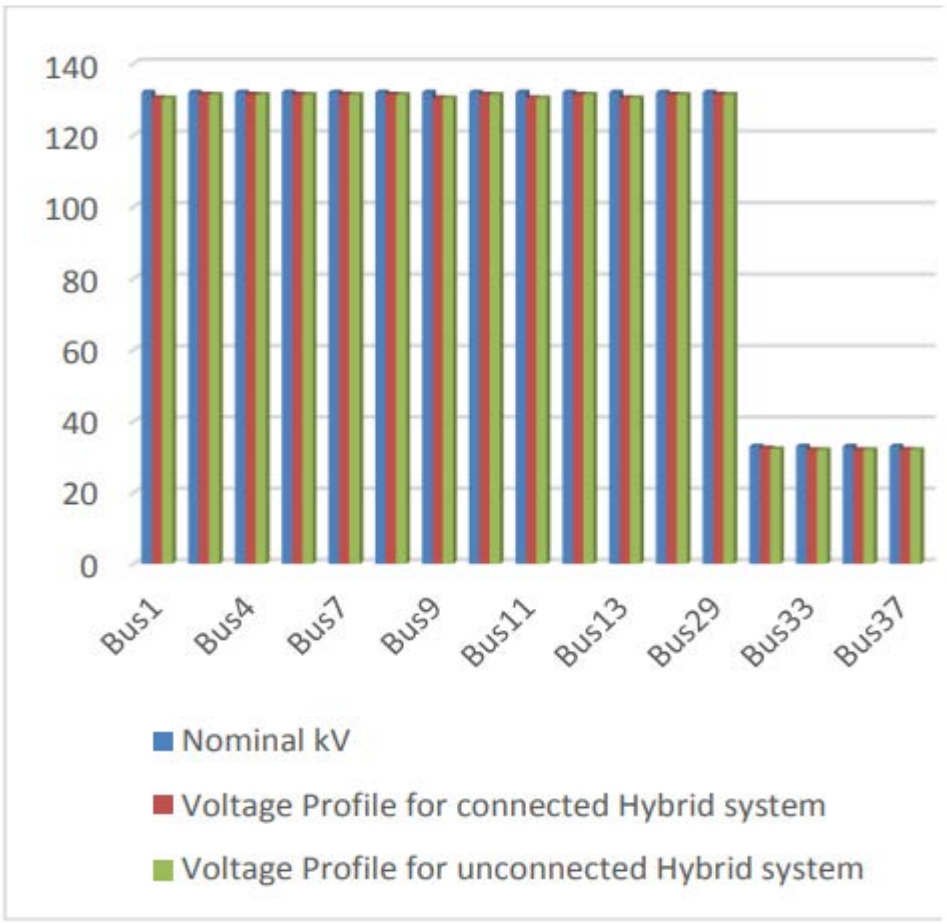

Figure 32. Un-connected and Connected Scenario at 33Kv Voltage Profile.

The chart indicates an enhancement in the voltage profile for specific buses labelled 1, 4, 7, 9,11, 13, and 29, within the network. These buses directly benefit from the connection to the hybrid system. On the other hand, buses that had no direct connection to the hybrid system experienced minimal changes in their voltage magnitude.

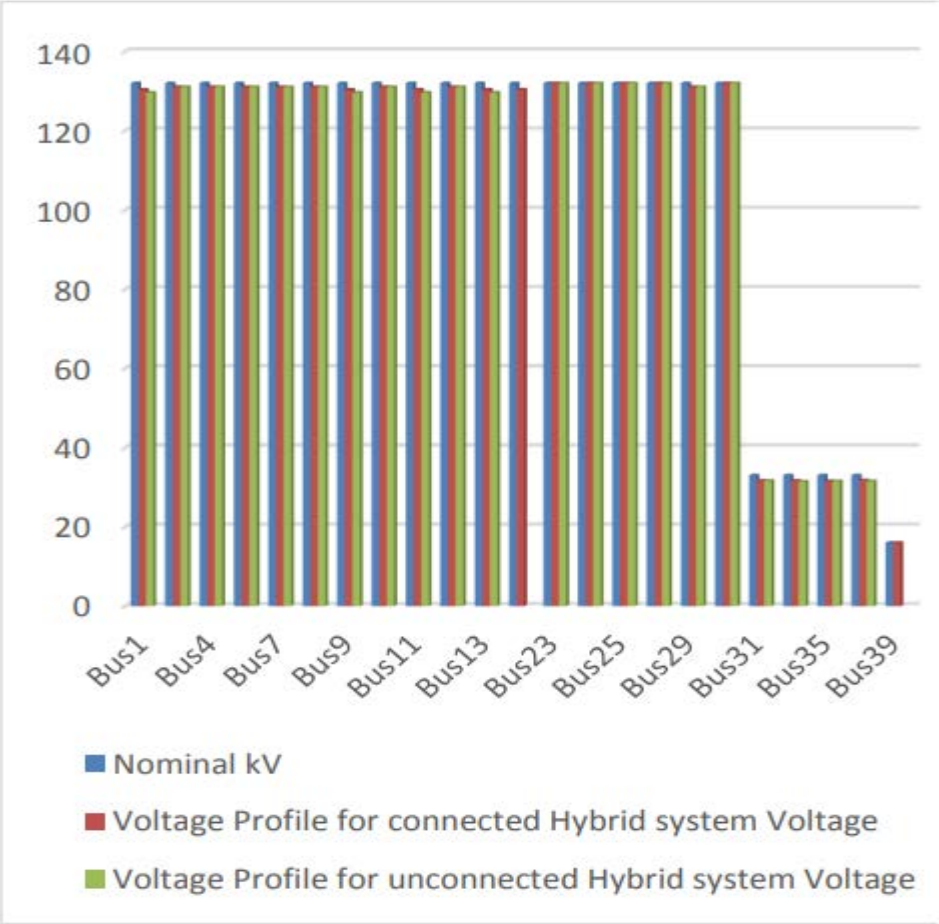

Figure 33. Connected and Unconnected voltage profile at 132kV

Voltage improvements were observed on buses 1, 9, 11, and 13, as these buses directly benefited from the connection to the hybrid system. However, other buses that had no direct connection to the hybrid system remained unchanged. In the unconnected system, no value was recorded for Bus 39 and Bus 23 because the hybrid system was linked to both buses for power evacuation to the grid, and in the unconnected simulation, they were not connected.

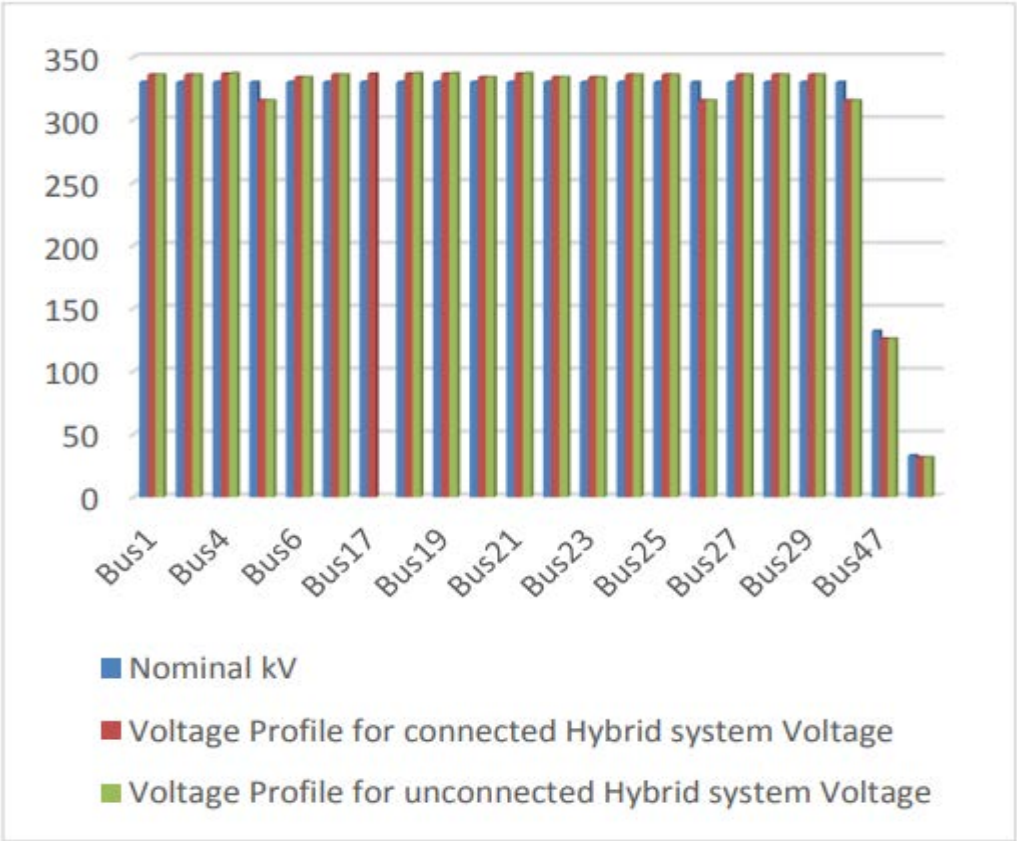

Figure 34. Connected and Unconnected voltage profile at 330kV

Based on the provided information, buses 4,19, and 21 experienced an improvement in voltage. Additionally, buses with the same voltage magnitude were observed, as they are connected to the same infinite bus. On the other hand, Bus 17 recorded no values in the unconnected system because it was connected to the hybrid system for power evacuation to the Grid and was not active in the unconnected scenario.

3. Scenario Two

The observed line losses for the Grid network were analysed for both the connected and un-connected Hybrid scenarios.

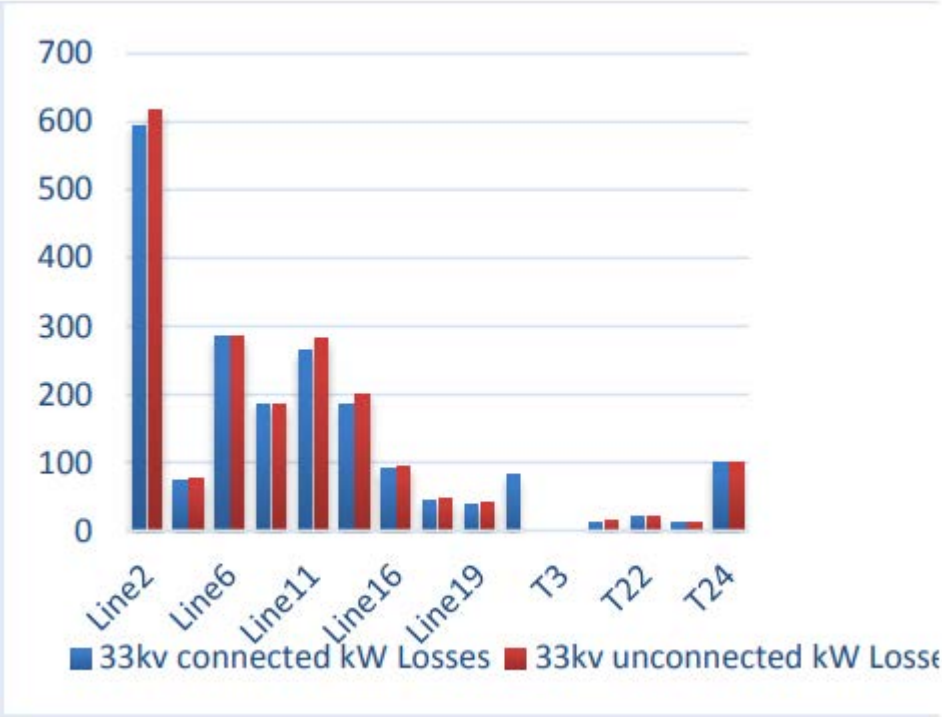

Figure 35. Connected and Un-Connected Scenario for 33kV Line Losses

Based on the above illustration, significant reductions in line losses were observed when the Hybrid system was connected to the 33kV line. This reduction is evident in Line 2, Line 6, Line 11, Line 16, Line 19, Transformer 22 on the chart. When compared to the unconnected Grid, the Hybrid system serves as a relief system to the existing grid, resulting in overall reduced losses within the system. No losses were recorded for the unconnected system in Transformer 3 because it was connected to the Hybrid system for power transmission to the grid. However, no noticeable difference was observed in Lines 6, as there was no connection between the buses and the hybrid system at this point.

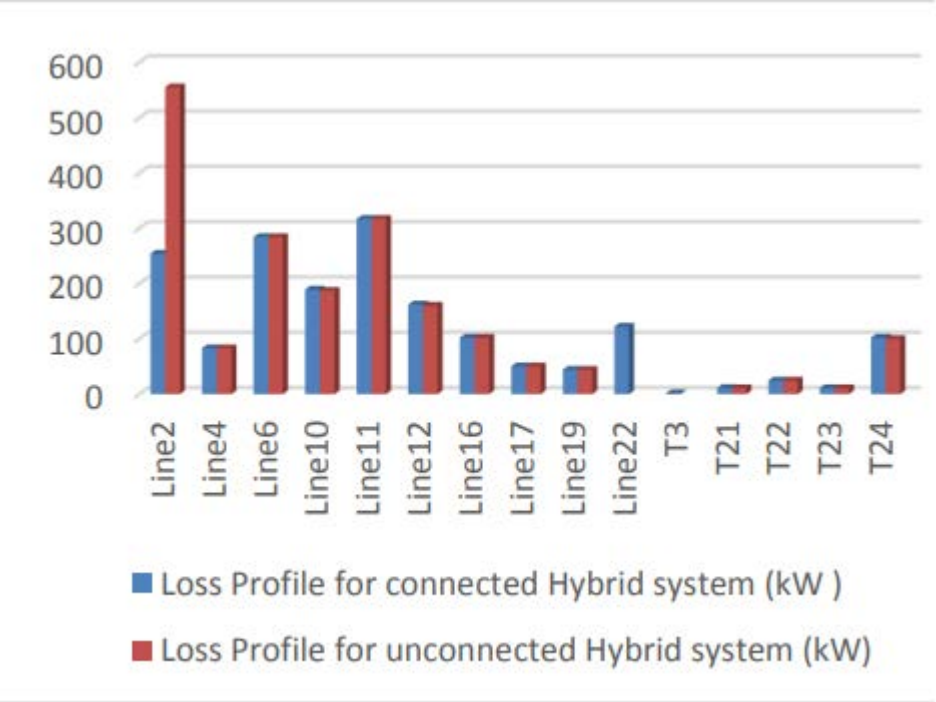

Figure 36. Connected and Un-Connected Scenario for 32 KV Line Losses

When the 132kV line was connected to the Hybrid System, Line 2 showed a notable reduction in losses. However, there was a substantial increase in losses observed in Line T21, T22, Line 12, and Line 10 when comparing the results to the simulation without the Hybrid System. On the other hand, no significant difference was observed in other lines because there was no connection between the hybrid system and the buses at those points.

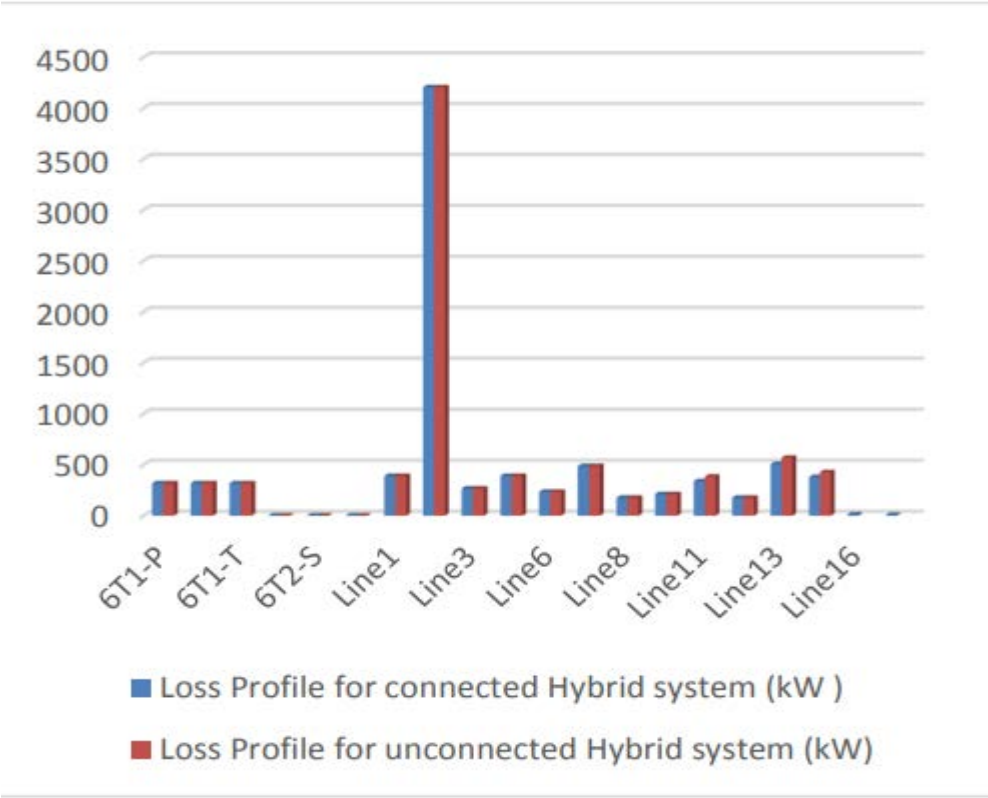

Figure 37. Connected Scenario and Un-Connected 330kV Line Losses

Lines 13, and 11 showed a slight reduction in losses when the Hybrid system was connected to the network, benefiting from the relief provided by the hybrid system. In contrast, Line 16 recorded no value in the unconnected system. This is because both lines were connected to the hybrid system for power evacuation to the Grid and were not active in the simulations conducted for the unconnected scenario.

4. Scenario Three

This involves studying the impact of a percentage load increase of 20%, 60%, and 100% on the hybrid-grid operating at 33kV. considering both connected and un-connected portions of the hybrid-grid system.

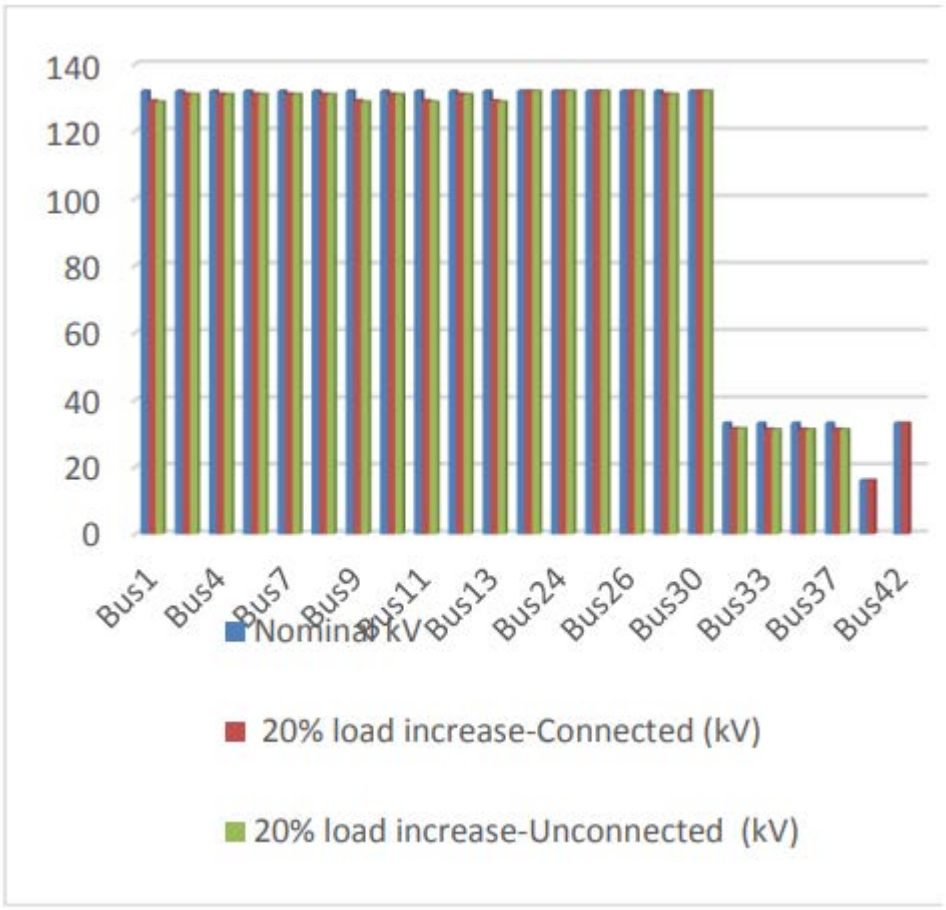

Figure 38. 33kV Line Voltage profile 20% Load Increase Chart

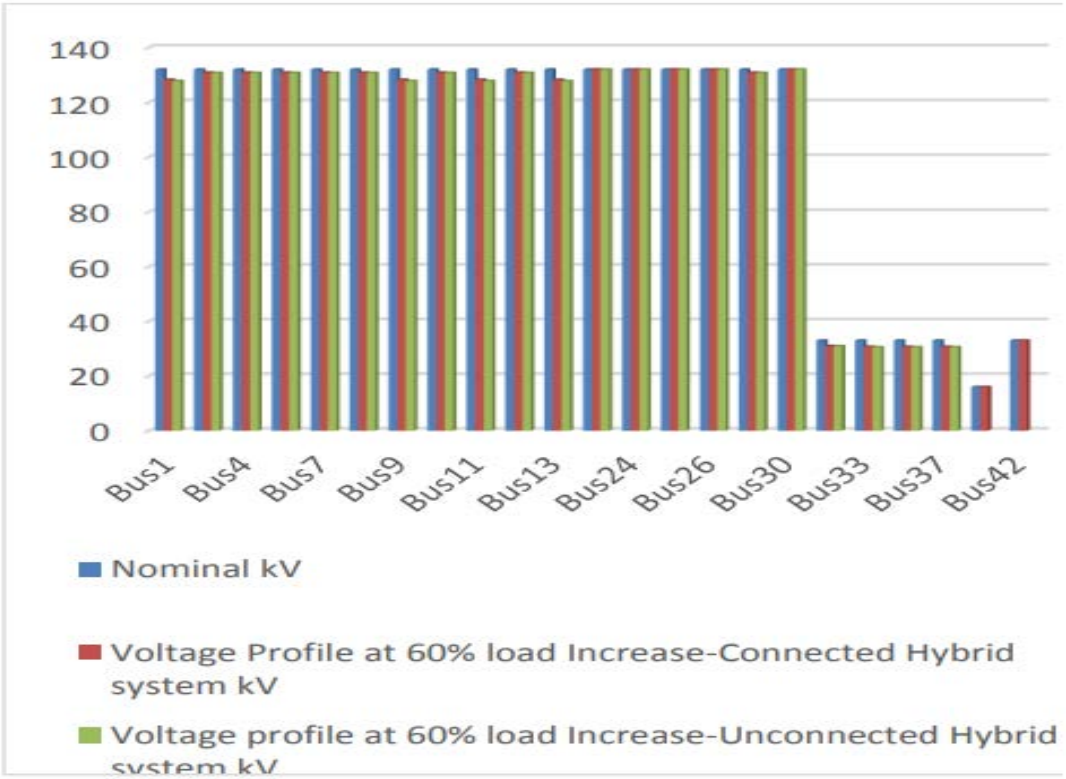

Figure 39. 33kV Line Voltage profile 60% Load Increase Chart

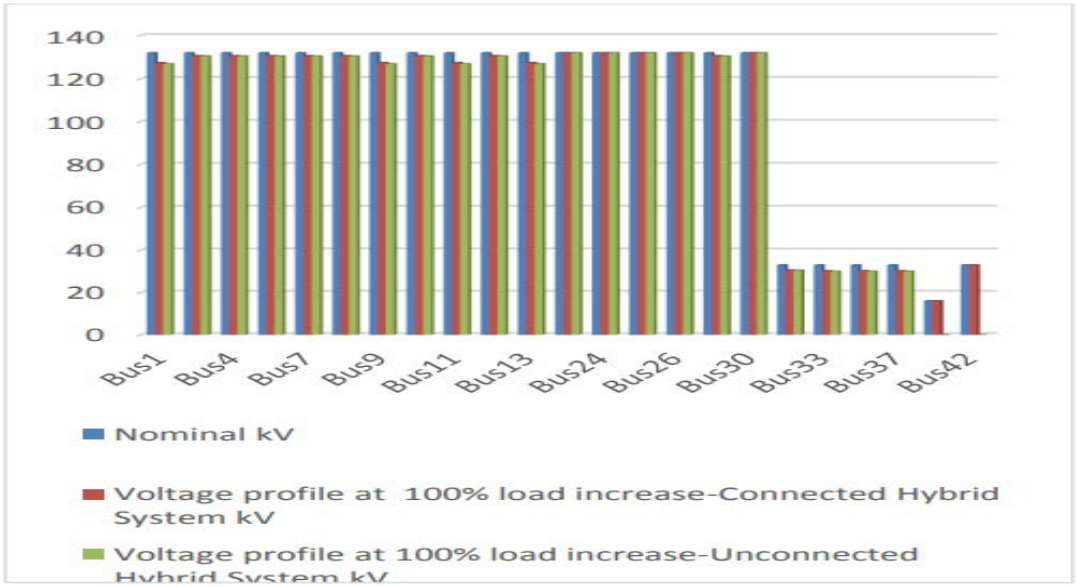

Figure 40. 33kV Line Voltage profile 100% Load Increase Chart

5. Summary

The assessment of power flow within the Nigerian power grid, operating at varying voltages of 330kV, 132kV, and 33kV, is of utmost importance to evaluate the network's capability in handling scheduled loads and fluctuations in power generation. The grid comprises 52 buses, 29 branches, 4 connected loads, and 7 transformers for the 330kV network, while the 132/33kV network consists of 24 buses, 23 branches, 9 connected loads, and 5 transformers. These specifications were utilized to gauge the impact of integrating a total of 40MW of hybrid generators (20MW from solar and 20MW from wind) into the grid network, with a generated voltage of 16kV. The selection of power generation was based on the overall load demand from the existing network, and the network model serves as a comprehensive tool to thoroughly assess the network's stability under steady-state conditions.

This project focuses on elucidating the wind and solar hybrid system with a DC load. Each energy source is connected to the local climate, taking into account variations in wind speed and radiation. To ensure maximum power delivery regardless of environmental changes, voltage and current sensors are installed for each source. The rationale behind choosing this Hybrid system lies in its reliability, especially during power cuts, as it combines two power sources. The system's autonomy is guaranteed by this combination, and it is connected to the Grid. Some of the Data used in this work was collected from external sources due to the fact that I

could not be physically present where this project would be located at the given time.

In this study various simulations were carried out, the voltage profile of the connected and unconnected Hybrid-Grid Network was analysed and compared, the observed line losses for the Grid network were analysed for both the connected and un-connected Hybrid scenarios and also the impact of a percentage load increase of 20%, 60%, and 100% on the hybrid-grid operating at 33kV. considering both connected and un-connected portions of the hybrid-grid system.

Figure 51 illustrates the relationship between the line-to-line output and time, providing valuable insights into the system's performance over time.

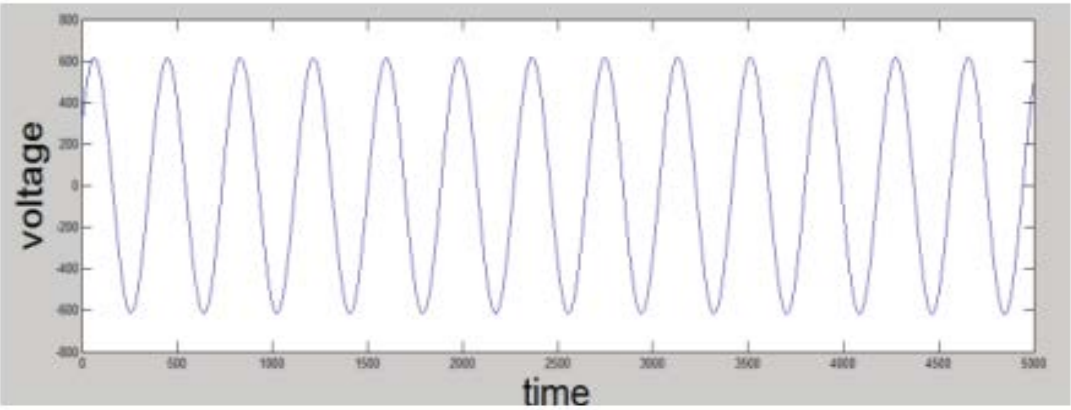

Figure 41. Line to line output voltage w.r.t. time

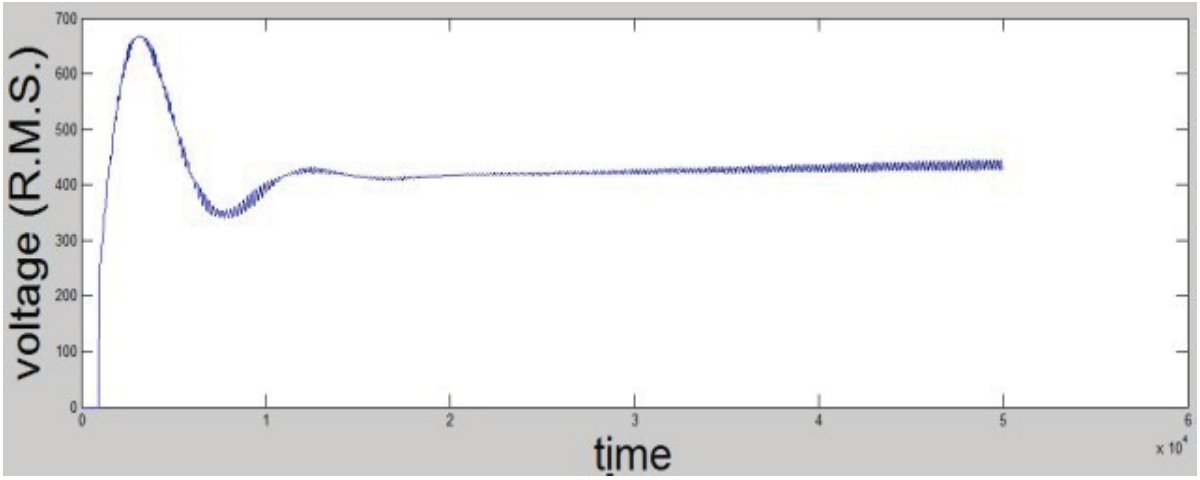

Figure 42. Rms voltage output and w.r.t. time

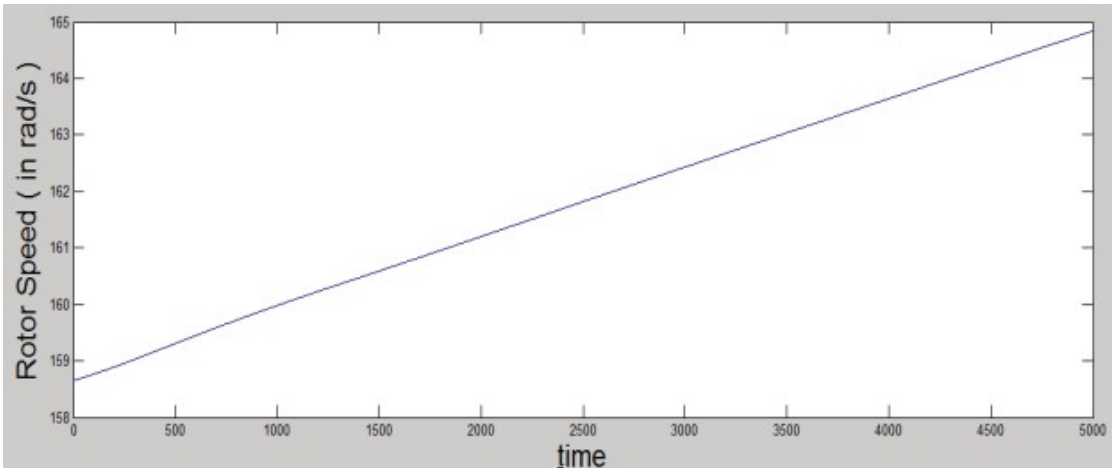

Figure 43. Variation of rotor speed with time

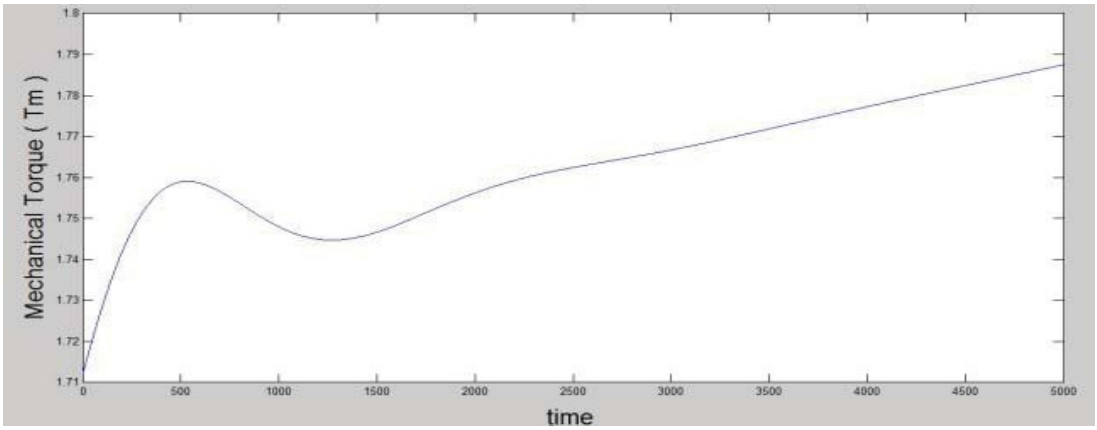

Figure 44. Output Voltage Characteristics of Solar Power Plant.

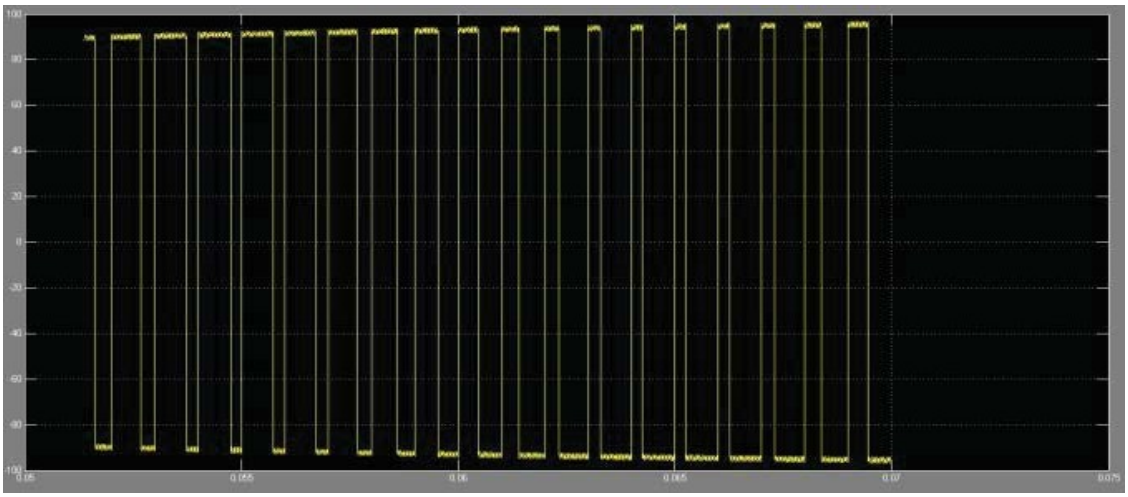

Figure 45. Output Voltage Characteristics of Solar Power Plant

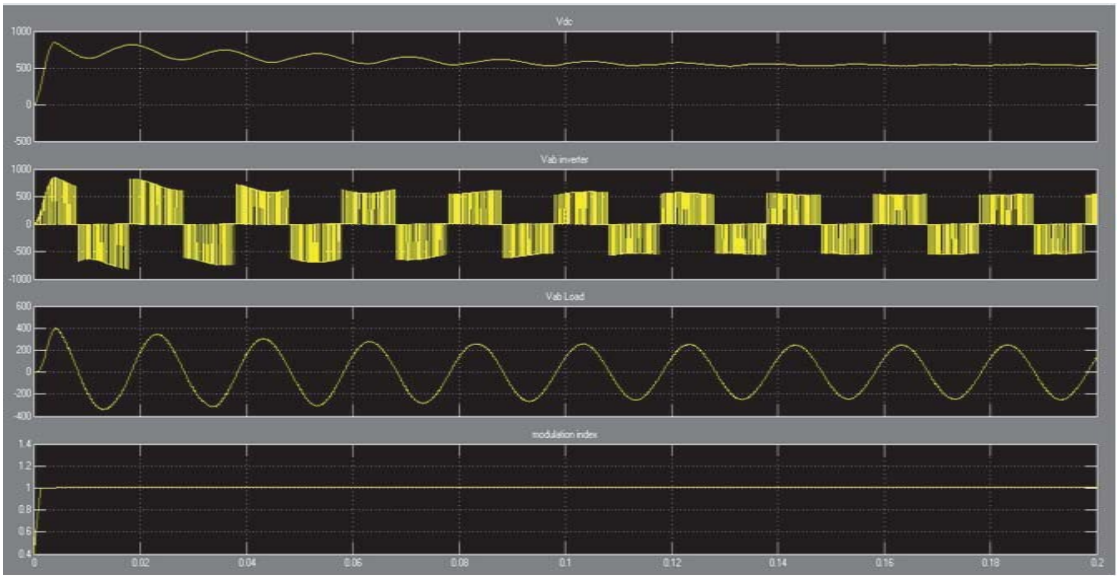

Figure 46. Hybrid system Output Simulink

VI. CONCLUSION

The results obtained from steady state analysis under different scenarios demonstrate that integrating the post-hybrid integrated network significantly improves power supply quality and reliability in the existing Nigerian grid, which operates at voltages of 330kV, 132kV, and 33kV. To evaluate the accuracy and responsiveness of the P&O MPPT method in tracking solar irradiation, the simulation used a step time of 0.1 and assumed irradiance levels ranging from 200 to 1000 W/m2. (the PV current variations observed over time, established by the Perturb and Observe (P&O) algorithm. Notably, the MPP is consistently and effectively reached in all cases, with minor oscillations persisting until the next switch in irradiance. The algorithm demonstrates a response time of 60 seconds, which is considered acceptable.)

The integration of the Hybrid Photovoltaic and Wind System (HPWS) has a substantial impact on both voltage levels and line losses of the interconnected lines associated with the hybrid system. Comparing the scenarios based on the voltage level at which the hybrid system is connected to the grid, This configuration results in the most favourable overall outcome with improved voltage profiles and significant reduction in line losses. The primary control loop was established based on the vector control loop, which played a critical role in stabilizing the DC output voltage. This stabilized voltage served as the primary energy source for supplying the grid with both active and reactive power. The obtained results strongly emphasized the significance of this control loop in attaining a stable current profile, which can be seamlessly injected into the grid.

In this study, a MATLAB simulation was conducted to assess the performance of a wind and solar energy system connected to the grid. A comprehensive outline of the crucial steps involved in simulating a grid-connected photovoltaic (PV) system. Additionally, detailed mathematical models for both the DC-DC boost converter and the DC-AC inverter, integrated with the PV array, have been presented. By employing the Perturb and Observe (P&O) algorithm, the

Maximum Power Point (MPP) is efficiently tracked, ensuring optimal energy generation from the PV array and minimizing losses. As a result, our primary objective has been successfully accomplished. Various output graphs were generated to showcase different parameters over time, including line-to-line voltage output, DC output from solar photovoltaic (PV) and the AC output from the inverter. Finally, the graph presents the output voltage of the hybrid system that combines solar and wind power.

VII. REFERENCES

BOOKS

A BHATI, M. HANSEN, AND C. M. CHAN, **"Energy conservation through smart homes in a smart city: A lesson for Singapore households,"** Energy Policy, vol. 104, no. January, pp. 230–239, 2017.

E. HOSSEINI, **"Modeling and Simulation of Choppers Switching Via Matlab/Simulink,"** Sci. Bull. Petru Maior Univ. Targu Mures, vol. 12, no. 1, 2015.

H. BELLIA, R. YOUCEF, AND M. FATIMA, "**A detailed modeling ofphotovoltaic module using MATLAB,**" NRIAG J. Astron. Geophys., vol. 3, no. 1, pp. 53–61, 2014.

H. REZK AND A. M. ELTAMALY, "**A comprehensive comparison ofdifferent MPPT techniques for photovoltaic systems,"** Sol. Energy, vol. 112, pp. 1–11, 2015.

L. QIN AND X. LU, **"Matlab/Simulink-Based Research on Maximum Power Point Tracking of Photovoltaic Generation,"** Phys. Procedia, vol. 24, pp. 10–18, 2012.

PANDA, M. K. PATHAK, AND S. P. SRIVASTAVA, **"A single phase photovoltaic inverter control for grid connected system,"** Sadhana, vol. 41, no. 1, pp. 15–30, 2016.

R. R. MOJUMDAR, M. SAKHAWAT, H. HIMEL, AND S. RAHMAN, **"Electric Machines & Their Comparative Study for Wind Energy Conversion Systems (WECSs),"** vol. 4, no. 4, 2016.

R. SHAFFER, **Fundamentals of Power Electronics with Matlab**. Firewall Media, 2013.

R. W. ERICKSON AND D. MAKSIMOVIC, **Fundamentals of power electronics**, Springer Science & Business Media, 2007.

ARTICLES

A KADRI, H. MARZOUGUI AND F. BACHA, "MPPT control methods inwind energy conversion system using DFIG," **2016 4th International Conference on Control Engineering & Information Technology (CEIT)**, 2016, pp. 1-6, doi: 10.1109/CEIT.2016.7929115. Kumar Pushpak,Priety and Vijay Kumar Garg, “To Perform Matlab Simulation of Battery

A SALEM, FARHAN, “Modeling and Simulation issues on PhotoVoltaicsystems, for Mechatronics design of solar electric applications,” **IPASJ Ineternational J. Mechnical Eng**., vol. 2, no. 8, pp. 24–47, 2014.

ANURADHA,SINHA, S. K., AND AKHILENDRA YADAV. "Modelling ofDC linked PV/hydro hybrid system for rural electrification." **2017 Recent Developments in Control, Automation & Power Engineering (RDCAPE)**. IEEE, 2017.

Charging Using Solar Power with Maximum Power Point Tracking(MPPT)”, **International Journal of Electronic and Electrical Engineering**. ISSN 0974-2174, Volume 7, Number 5 (2014).

F ADAMO, F. ATTIVISSIMO, A. DI NISIO, A. M. L. LANZOLLA, AND M.SPADAVECCHIA, “Parameters Estimation for a Model of Photovoltaic Panels,” **XIX IMEKO World Congr. Fundam. Appl. Metrol. Lisbon, Port**., 2009.

G CELSA AND G. M. TINA, “Matlab/Simulink model of photovoltaicmodules/strings under uneven distribution of irradiance and temperature,” **in 6th International Renewable Energy Congress**, IREC 2015, 2015.

G. WALKER,” MPPT converter topologies using a MATLAB PVmodel”,**Journal of Electrical & Electronics Engineering, Australia**, 2001;Vol.21, No. 1,49-56.

H. TSAI, C. TU, AND Y. SU, “Development of Generalized Photovoltaic Model Using MATLAB / SIMULINK,” **Proc. World Congr. Eng. Comput.**

Sci., 2008.

HARDIK K MEHTA, DR. VINOD KUMAR YADAV," Wind-PV HybridSystem with MPPT Control", **International Journal for Advance Research in Engineering and Technology**, Volume 2, Issue VII July 2014 ISSN 2320-6802.

J. RAMOS HERNANZ, J. J. CAMPAYO MARTÍN, I. ZAMORA BELVER, J.LARRAÑAGA LESAKA, E. ZULUETA GUERRERO, AND E. PUELLES PÉREZ, "Modelling of photovoltaic module," **Int. Conf. Renew. Energies Power Qual. Granada, Spain**, vol. 1, no. 8, 2010.

KAVITHA SIRASANI, S.Y. KAMDI ,"Solar Wind Hydro Hybrid EnergySystem Simulation", **International Journal of Soft Computing and Engineering (IJSCE)** ISSN: 2231-2307, Volume-2, Issue-6, January 2013.

L. S. C. KUMAR AND K. PADMA, "Matlab/Simulink Based Modelling andSimulation of Residential Grid Connected Solar Photovoltaic System," **Int. J. Eng. Res. Technol**., vol. 3, no. 3, 2014.

M. ASSAF, D. SESHSACHALAM, D. CHANDRA, AND R. K. TRIPATHI,"Dc- dc converters via matlab/simulink," **Proc WSEAS Conf. Autom. Control. Model. Simul. (ACMOS'05), Prague, Czech Repub**., pp. 464–471, 2005.

M. C. ARGYROU, P. CHRISTODOULIDES, C. C. MAROUCHOS, AND G.A. FLORIDES, "Energy storage technologies, nearly Zero Energy Buildings and a short-term storage application," **in 5th International Conference on Renewable Energy Sources & Energy Efficiency** - New Challenges, 2016.

M. C. ARGYROU, P. CHRISTODOULIDES, C. C. MAROUCHOS, S. A.KALOGIROU, G. A. FLORIDES, AND L. LAZARI, "Overview of Energy Storage Technologies and a Short-term Storage Application for Wind Turbines," **in the 26th International Ocean and Polar Engineering Conference**, 2016.

M. G. VILLALVA, J. R. GAZOLI, AND E. R. FILHO, "Comprehensiveapproach to

modeling and simulation of photovoltaic arrays," **IEEE Trans. Power Electron.**, vol. 24, no. 5, pp. 1198–1208, 2009.

M. S. DRESSELHAUS AND I. L. THOMAS, "Dresselhaus," **J. EnergyResour. Technol**., vol. 414, no. November, 2001.

MATLAB / SIMULINK," **Int. J. Comput**. **Appl**., vol. 31, no. 6, 2011.

N. A. ZAINAL, AJISMAN, AND A. R. YUSOFF, "Modelling of Photovoltaic Module Using Matlab Simulink," **in IOP Conference Series: Materials Science and Engineering**, 2016, vol. 114, no. 1.

N. FEMIA, G. PETRONE, G. SPAGNUOLO, AND M. VITELLI,"Optimization of Perturb and Observe Maximum Power Point Tracking Method," **IEEE Trans. Power Electron.,** vol. 20, no. 4, pp. 963–973, 2005.

N. M. A. A. SHANNAN, N. Z. YAHAYA, AND B. SINGH, "Single-DiodeModel and Two-Diode Model of PV Modules: A Comparison," **Proc. - 2013 IEEE Int. Conf. Control Syst. Comput. Eng. ICCSCE** 2013, pp. 210–214, 2013.

N. PANDIARAJAN AND R. MUTHU, "Mathematical Modeling of Photovoltaic Module with Simulink," **Int. Conf. Electr. Energy Syst.** (ICEES 2011), 2011.

OBAIDULLAH LODIN, NITIN KHAJURIA, SATYANANDVISHWAKARMA, GAZIA, " Modeling and Simulation of Wind Solar Hybrid System using Matlab/Simulink". **International Journal of Innovative Technology and Exploring Engineering** (IJITEE) ISSN: 2278-3075, Volume-8.

R. B. A. KOAD, A. F. ZOBAA, AND A. EL-SHAHAT, "A Novel MPPTAlgorithm Based on Particle Swarm Optimization for Photovoltaic Systems," **IEEE Trans. Sustain. Energy,** vol. 8, no. 2, pp. 468–476, 2017.

S. M. A. FAISAL, "Model of Grid Connected Photovoltaic System Using

S. NEMA, R. K. NEMA, AND G. AGNIHOTRI, "Matlab / simulink based study of photovoltaic cells / modules / array and their experimental verification," **Int. J. Energy Environ**., vol. 1, no. 3, pp. 487–500, 2010.

S. S. RAGHUWANSHI AND K. GUPTA, "Modeling of a single-phase grid-

connected photovoltaic system using MATLAB/Simulink," **in IEEE International Conference on Computer Communication and Control**, IC4 2015, 2015.

S. UMASHANKAR, K. P. APARNA, R. PRIYA, AND S.SURYANARAYANAN, "Modeling and Simulation of a PV System using DC-DC Converter," **Int. J. Latest Res. Eng. Technol**., vol. 1, no. 2, pp. 9– 16, 2015.

SUBUDHI AND R. PRADHAN, "A Comparative Study on Maximum Power Point Tracking Techniques for Photovoltaic Power Systems," **IEEE Trans. Sustain. Energy**, vol. 4, no. 1, pp. 89–98, 2013.

T. ESRAM AND P. L. CHAPMAN, "Comparison of Photovoltaic Array Maximum Power Point Tracking Techniques," **IEEE Trans. Energy Convers**., vol. 22, no. 2, pp. 439–449, 2007.

Z. SABIRI, N. MACHKOUR, M. B. CAMARA, AND B. DAKYO, "DC / DCconverters for Photovoltaic Applications- Modeling and Simulations," **in International Renewable and Sustainable Energy Conference (IRSEC)**, 2014, pp. 209–213.

ENCYCLOPEDIAS

DAVE FREEMAN," Introduction to Photovoltaic Systems Maximum Power Point Tracking," **Texas Instruments, Application Report**, SLVA446– November 2010.

LUXOR, "Photovoltaic module Eco Line 60/230-250W, LX-250P.

UNIVERSITY OF COLORADO, "ECEN2060 MATLAB/Simulink materials," **2012.[Online].Available:http://ecee.colorado.edu/~ecen2060/matlab.html**. [Accessed: 01- May-2017].

DISSERTATIONS

H. B. VIKA, "Modelling of Photovoltaic Modules with Battery Energy Storage in Simulink / Matlab," Master dissertation, Norwegian Univ. of Science and Technology (NTNU), 2014.

P. I. MUOKA, “Control of Power Electronic Interfaces for Photovoltaic Power Systems for Maximum Power Extraction,” Ph.D dissertation, University of Tasmania, 2014.

RESUME

Eromosele Oziegbe IHONGBE

EDUCATION AND TRAINING

Master of Science in Energy Technology

Istanbul Aydin University (28/09/2021-Current)

Field(s) of Study: Energy Technology, Solar and wind Based Energy systems, Electrical Engineering, Mechanical Engineering.

Bachelors in Electrical Engineering(B.ENG)

Ambrose Alli University Ekpoma Edo state, Nigeria

Field(s) of Study: Electrical Electronics Engineering, Networking.

Certification in Sales and Marketing

Aniibol Consulting Group

West African senior school Certificate Exam (Waec)

Ambrose Alli University Secondary School (2008)

WORK EXPERIENCE

TECHNICIAN

FEDEX EXPRESS (2013-2015)

Department: Information Technology (I.T)

TECHNICIAN/ONLINE MARKETING MANAGER

ELO-EX TRANSPORT SERVICE (2016/2020)

DIGITAL SKILLS

Internet User/Gmail/Computer Literacy/ Microsoft Office user.

SOCIAL SKILLS

Friendly/Decision Making/ Good Listener and Communicator/Team work/ Self-Motivation/Hard working/Flexible Responsible, I can also work under pressure.

REFEREES

Professor

Name: Professor.Dr. Mehmet Emin Tacer

Thesis Supervisor at Istanbul Aydin University.

Banker

Name: Negbenose Osemudiamen

Banker at Zenith Bank of Nigeria and Mentor.